



Akademie věd České republiky

Teze doktorské disertační práce
k získání vědeckého titulu "doktor věd"
ve skupině technických věd

**STRESS RIBBON AND CABLE SUPPORTED
PEDESTRIAN BRIDGES**

Komise pro obhajoby doktorských disertací v oboru mechanika těles,
konstrukcí, mechanismů a prostředí

Prof. Ing. Jiří Stráský, CSc.

Vysoké učení technické v Brně, Fakulta stavební, Ústav betonových a zděných konstrukcí

Brno, únor 2006

CONTENTS

1	INTRODUCTION.....	3
2	STRUCTURAL SYSTEMS.....	4
3	CABLE ANALYSIS.....	11
4	STRESS RIBBON STRUCTURES.....	15
4.1	Structural arrangement.....	15
4.2	Static function.....	18
4.3	Static Analysis.....	20
4.4	Dynamic analysis.....	24
4.5	Example of the analysis.....	25
4.6	Stress ribbon supported by arch.....	26
4.7	Static and dynamic loading tests.....	28
5	SUSPENSION STRUCTURES.....	29
5.1	Structural arrangement.....	29
5.2	Static and dynamic analysis.....	30
5.3	Example of the analysis.....	32
6	CABLE STAYED STRUCTURES.....	33
6.1	Structural arrangement.....	33
6.2	Static Analysis.....	33
6.3	Redistribution of stresses.....	35
6.4	Restricting of the horizontal movement.....	38
7	CONCLUSIONS.....	39
	REFERENCES.....	39

1 INTRODUCTION

'What would be the best bridge? Well, the one which could be reduced to a thread, a line, without anything left over; which fulfilled strictly its function of uniting two separated distances.'

Pablo Picasso



Fig.1.1 – Redding Pedestrian Bridge



Fig.1.2 – Vranov Lake Pedestrian Bridge

Stress-ribbon bridge is the term that has been coined to describe structures formed by directly walked prestressed concrete deck with the shape of a catenary [18],[23],[28]. The bearing structure consists of slightly sagging tensioned cables, bedded in a concrete slab that is very thin compared with the span. This slab serves as a deck, but apart from the distributing the load locally and preserving the continuity, it has no other function. It is a kind of suspension structure where the cables are tensioned so tightly that the traffic can be placed directly on the concrete slab embedding the cables. Compared with other structural types the structure is extremely simple. On the other hand, the force in the cables is very large making the anchoring of the cable expensive.

From Fig.1.1 it is evident that the stress ribbon structure represents the simplest structural form. Such structures can be either cast in-situ or formed of precast units. In the case of precast structures, the deck is assembled from precast segments that are suspended on bearing cables and shifted along them to their final position. Prestressing is applied after casting the joints between the segments to ensure sufficient rigidity of the structures.

In the course of time people have realized that the decks can be suspend on the cables of larger sag and in this way it is possible to reduce tensions in the cables. The first suspension structures had flexible decks that were in some cases stiffened by a net of additional cables. It was J. Finley [5], who first identified the major components of suspension bridges: a system comprising main cables from which a deck braced by trusses was hung.

The problem of vibration and even overturning of light pedestrian suspension structures due to wind load was well documented [13]. However, the failure of the Tacoma Bridge has drawn the attention of engineers to the aerodynamics stability of suspension structures [15]. Therefore new suspension structures have a deck formed by an open stiffened steel truss of sufficient torsional and bending stiffness [4] or use a streamlined steel box girder [12].

Another approach to providing stiffness is to construct a slender concrete deck and stiffen the structure by a system of inclined suspenders [16]. This approach has been successfully developed and erected from designs by Professor J. Schlaich. Slenderizing the deck could be combined with techniques often used to stabilize utility bridges. In such cases, the concrete deck is stiffened by the post-tensioning of external cables with an opposite curvature to that of the main suspension cables. Similar effects can be achieved by eliminating the longitudinal movement of the deck. The combination of the stiffening of the deck by external cables situated within the deck and



Fig.1.3 – Model test

eliminating of the horizontal movement was used in the design of the Vranov Lake Bridge (see Fi.1.2) built in 1993 in the Czech Republic [25]. The deck of the span $l = 252$ m is assembled of precast concrete segments of depth of only $d = 0.40$ m. The bridge deck with the ratio $d/l = 1/630$ is one of the most slender structures ever built.

While suspension structures have been widely designed both in the nineteenth and twentieth century, the development of modern cable supported structures have started after the Second World War. It was Prof. F. Dishinger, who first emphasized the importance of high initial stress in the stay cables and designed the first modern cable-stayed bridge built in Strömsund, Sweden in 1955. Since then

many cable-stayed structures with both steel and concrete decks have been constructed [5], [7], [9], [10], [13]. The development of the prestressed concrete technology has significantly contributed to the development of the cable stayed structures. Prof. R. Walther has proved that a deck of average depth of 450 mm can be safely used for bridges with spans up to 200 m [32].

Although the above structures have a very simple shape, their design is not straightforward. It requires a deep understanding of structural forms, the functions of structural details and the behaviour of prestressed concrete structures post-tensioned by internal and/or external tendons. Also the static and dynamic analyses require an understanding of the function of cables and resolves various problems in regard to both geometric and material non-linearity.

2 STRUCTURAL SYSTEMS

The beauty of the suspension and arch structures comes from their economic structural shape [22]. Their economy is evident from Fig.2.1a that shows the trajectories of principal stresses in a uniformly loaded simply supported beam. From the figure it is evident that the maximum stresses occur only at the mid-span section and only in the top and bottom fibers. The beam has a

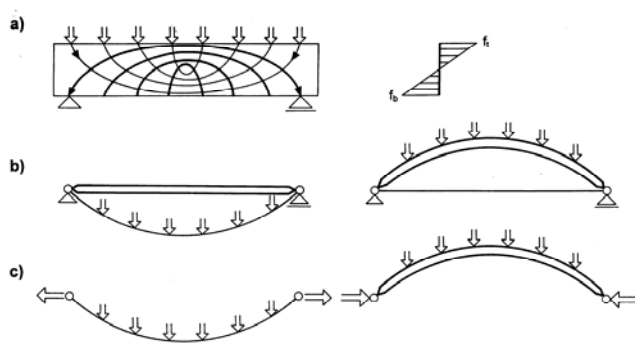


Fig.2.1 – Cable and arch structure

significant amount of dead mass that does not contribute at all to resisting the external loads.

From the figure it is clear that if we want to reduce the weight of the beam we have to eliminate as much dead mass as possible and utilize the tension or compression capacities of the structural members. From the beam we can derive a suspension cable or an arch in which the horizontal force is resisted by an internal strut or tie – see Fig.2.1b; in the case where the foundations are capable of resisting horizontal forces, we can substitute the strut or the tie by stiff

footings – see Fig.2.1c.

A uniformly loaded concrete arch can span several kilometers and a suspension cable can span even more. But their shape has to be funicular to the given load and the structures need to have an economic rise or sag.

The layout of pedestrian bridges is influenced by two requirements. In cable supported structures, where the deck follows the shape of the cables, only limited slope with corresponding sag can be accepted. Furthermore, these bridges need to have sufficient stiffness that guarantees comfortable walking and the stability of the shape – see Fig.2.2. It is therefore necessary to stiffen them.

The deformation of the suspension structures (see Fig.2.4a) can be reduced by stiffening the cables using dead load (see Fig. 2.4b), by external cables (see Fig.2.4c) or by creating a prestressed concrete band with a certain amount of bending stiffness to guarantee the distribution of local loads and the stability of the overall shape (see Figs.2.3 and 2.4d).

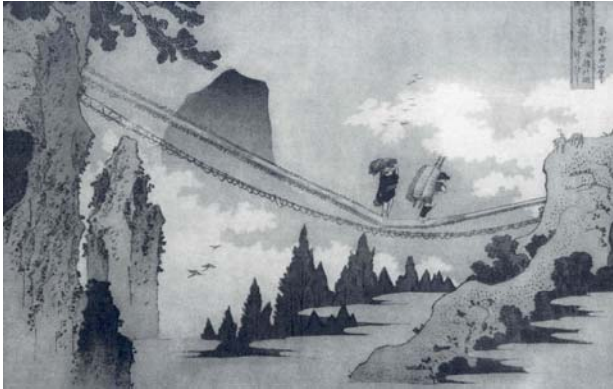


Fig.2.2 – Hokusai Bridge



Fig.2.3 – Prague-Troja Bridge - Loading test

Alternatively, cable supported structures can be stiffened by beams that distribute the load and give stability to the system (see Fig.2.5). In this way a suspension system formed by beams and suspension cables of economic sags can be developed (see Fig.2.5a, 2.5c). The suspension cables could also be substituted by a system of stay cables – see Fig.2.5b and 2.5d.

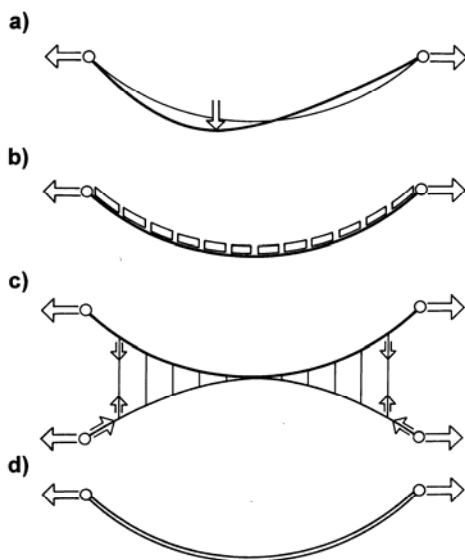


Fig.2.4 – Cable stiffening

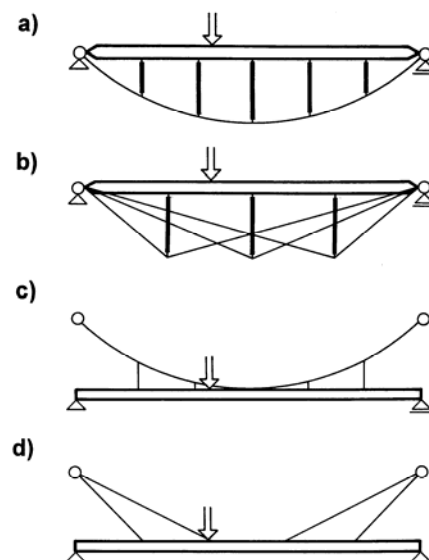


Fig.2.5 – Beam stiffening of the cable

When we think about a suspension structure, we usually assume that the cable is loaded at several points between the anchor points; when we imagine a cable-stayed structure, we assume that the cables are loaded only at their anchor points.

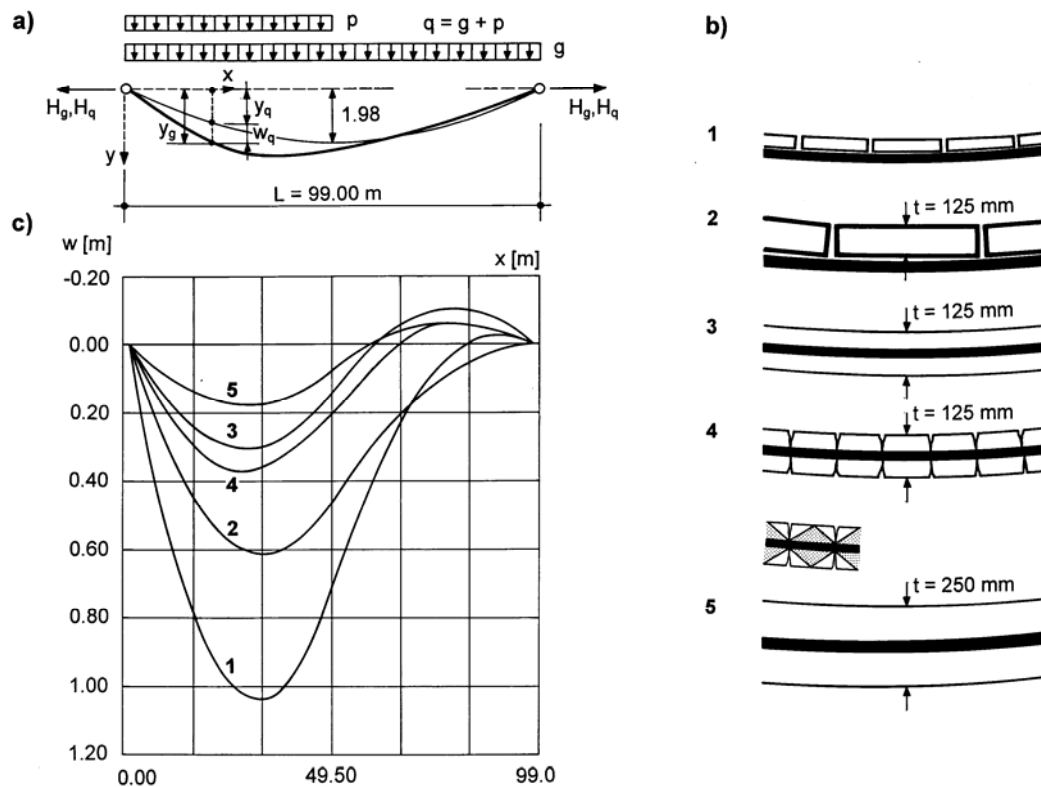


Fig.2.6 – Stiffness of the stress ribbon structure

If the suspension cables are situated above the deck, the load is transferred from the deck into the cables by tensioned hangers. In structures with cables situated under the deck the load is transferred from the deck into the cables by compression struts. The suspension and stay cables can be anchored outside of the stiffening beam in anchor blocks transferring the force from the cables into the soil or they can be anchored in the beam and create a so called self-anchored system. In the latter case, the footings are stressed by vertical reactions only.

The importance of the stiffening of directly walked suspension structures shown in Fig.2.4 is evident from the Fig.2.6 in which four stress ribbon structures are compared. Fig.2.6 shows a bridge of the span 99 m span with a maximum dead load slope of 8%, which yields maximum sag at mid-span of 1.98 m. The bridge is formed:

1. by two cables on which timber boards are placed. The total area of the cables is $A_s = 0.0168 \text{ m}^2$. The dead load $g = 5 \text{ kN/m}$ and the horizontal force $H_g = 3,094 \text{ kN}$,
2. by two cables that support concrete panels of 125 mm thickness. The total area of the cables is $A_s = 0.0252 \text{ m}^2$,
3. by a concrete band of 125 mm thickness that is supported by two cables. The total area of the cables is $A_s = 0.0252 \text{ m}^2$. The cables are embedded in the band that is fully prestressed and therefore uncracked,
4. by a concrete band of 125 mm thickness that is supported by two cables. The total area of the cables is $A_s = 0.0252 \text{ m}^2$. The cables are embedded in the band that is partially prestressed and therefore cracks can form in the concrete. It is assumed that the crack spacing is 125 mm and that the concrete between cracks resists resistance of the tension. The area of concrete that resists the tension to taken as $A_{c,cr} = \frac{1}{2} A_c$ as shown in Fig.2.6-4,
5. by a concrete band of 250 mm thickness that is supported by two cables. The total area of the cables is $A_s = 0.0392 \text{ m}^2$. The cables are embedded in the band that is fully prestressed and therefore uncracked.

Structures 2 through 4 are stressed by a dead load $g=17$ kN/m with corresponding horizontal force $H_g = 10,519$ kN. Structure 5 is stressed by a dead load $g=33.35$ kN/m with corresponding horizontal force $H_g = 20,635$ kN.

The above structures were analysed for the effects of the dead load g and live load $p=20$ kN/m placed on one half of the structure. The analysis was performed for the structure modeled as a cable of effective tension stiffness $E_s A_e$ and zero bending stiffness. The effective stiffness $E_s A_e$ was determined from the modulus of elasticity of the cable $E_s = 195,000$ MPa and an effective area A_e that depends on the area of the cable A_s and concrete band A_c (or $A_{c,cr}$ respectively) as well as the ratio of the modulus of elasticity of steel E_s and concrete E_c .

Resulting deformations of the structures are presented at Fig.2.6c. From the results it is evident that the fully prestressed band of thickness of 250 mm has the smallest deformations. Also fully and partially prestressed structures have reasonable deformations. It is evident that the prestressed concrete deck (fully or partially prestressed) has a superior behaviour. The monolithic concrete deck gives the structure not only a sufficient tension stiffness, but its membrane stiffness also guarantees the transverse stiffness of the bridge. These structures are further called *stress ribbon* structures. Stiffening of the suspension structures by a tension cable of opposite curvature (see Fig.2.4c) has similar effects to the stiffening of the structure by dead load (see Fig.2.4b).

The above analysis was done for the structure without considering the bending stiffness. To

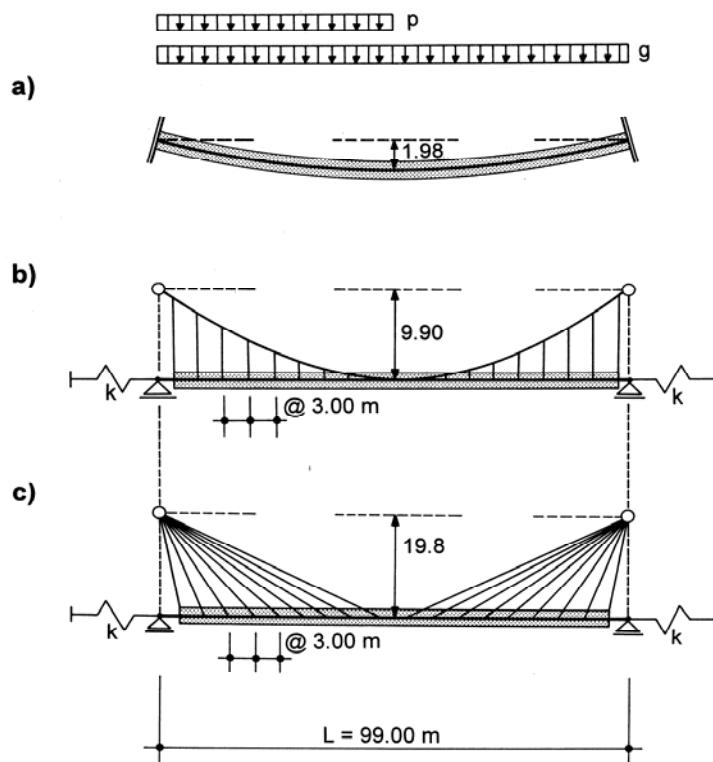


Fig.2.7 – Studied structures

$$\begin{aligned}
 I_c(1) &= 6.51 \text{ E-3 m}^4, & I_c(2) &= 1.00 \text{ E-2 m}^4, & I_c(3) &= 5.00 \text{ E-2 m}^4, & I_c(4) &= 1.00 \text{ E-1 m}^4, \\
 I_c(5) &= 5.00 \text{ E-1 m}^4, & I_c(6) &= 1.00 \text{ E-0 m}^4, & I_c(7) &= 5.00 \text{ E-0 m}^4, & I_c(8) &= 1.00 \text{ E+1 m}^4, \\
 I_c(9) &= 5.00 \text{ E+1 m}^4, & I_c(10) &= 1.00 \text{ E+2 m}^4.
 \end{aligned}$$

understand the influence of the bending stiffness of the prestressed band extensive studies on the one span structure were performed – see Fig.2.7a. The structure of span $L = 99.00$ m and sag $f = 1.98$ m ($f=0.02 L$) was developed from Structure No. 5 shown in Fig.2.6. The deck of a constant area but different bending stiffness was analysed for several positions of the live load and for the effects of temperature changes. From all the results only deformation, bending moments and normal force for two loadings are presented in Figs.2.8 and 2.9.

A concrete band of the area $A_c = 1.25 \text{ m}^2$ having a modulus of elasticity $E_c = 36,000$ MPa was assumed.

The analysis was performed for the following values of the moment of inertia:

The band was suspended on bearing tendons of total area $A_s = 0.0392 \text{ m}^2$ and modulus of elasticity $E_s = 195,000 \text{ MPa}$. The band had a constant area and therefore the dead load was also constant. Its value including the weight of bearing tendons was $g = 33.35 \text{ kN/m}$. The initial stresses in the bearing tendons were derived from the horizontal force:

$$H_g = \frac{gL^2}{8f} = \frac{33.35 \times 99.00^2}{8 \times 1.98} = 20,635 \text{ kN}$$

The structure was analysed as a 2D geometrically non-linear structure with the program system *ANSYS*. In the analysis both large deformations and the so called tension stiffening were considered. Figure 2.8 shows the deformation $w(x)$ and bending moments $M(x)$ along the length of the bridge, for loading by dead load and live load $p = 20.00 \text{ kN/m}$ situated on only one half of the structure. Also the values of the normal force in the bearing tendons and in the concrete deck at the mid-span section as a function of its bending stiffness are presented there.

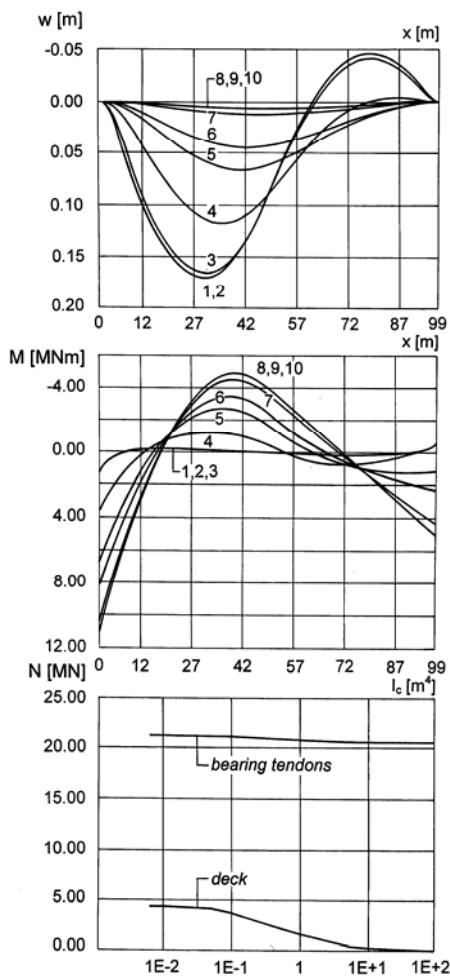


Fig.2.8 – Effects of the live load

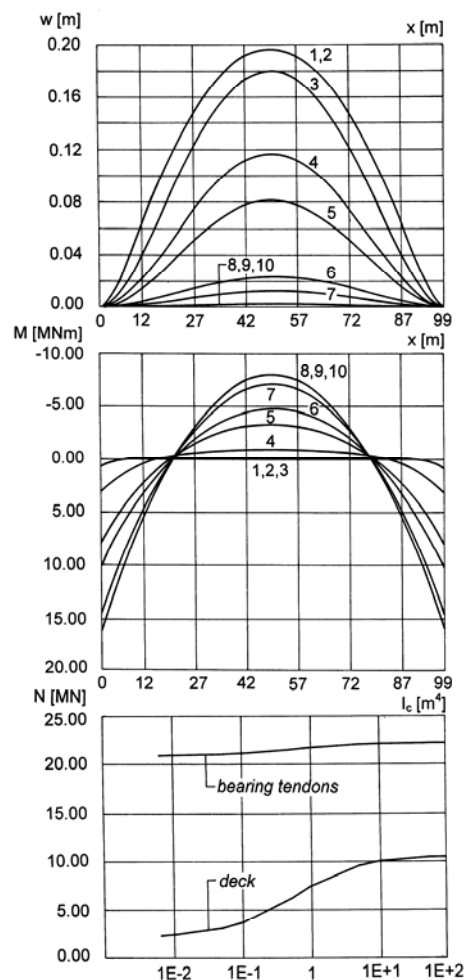


Fig.2.9 – Effects due to temperature drop

The same results for loading by dead load and temperature drop of $\Delta T = -20^\circ\text{C}$ are presented in Fig.2.9. From the figures it can be seen how the deformations and bending moments depend on the stiffness of the deck. It is evident that in the range of bending stiffness from $6.51 \text{ E-}3 \text{ m}^4$ to $5.00 \text{ E-}2 \text{ m}^4$ the deformation and bending moments are nearly the same. The structure resists the load by its tension stiffness and not by its bending stiffness. The deformations and normal forces are nearly the same as the ones for the cable without bending stiffness.

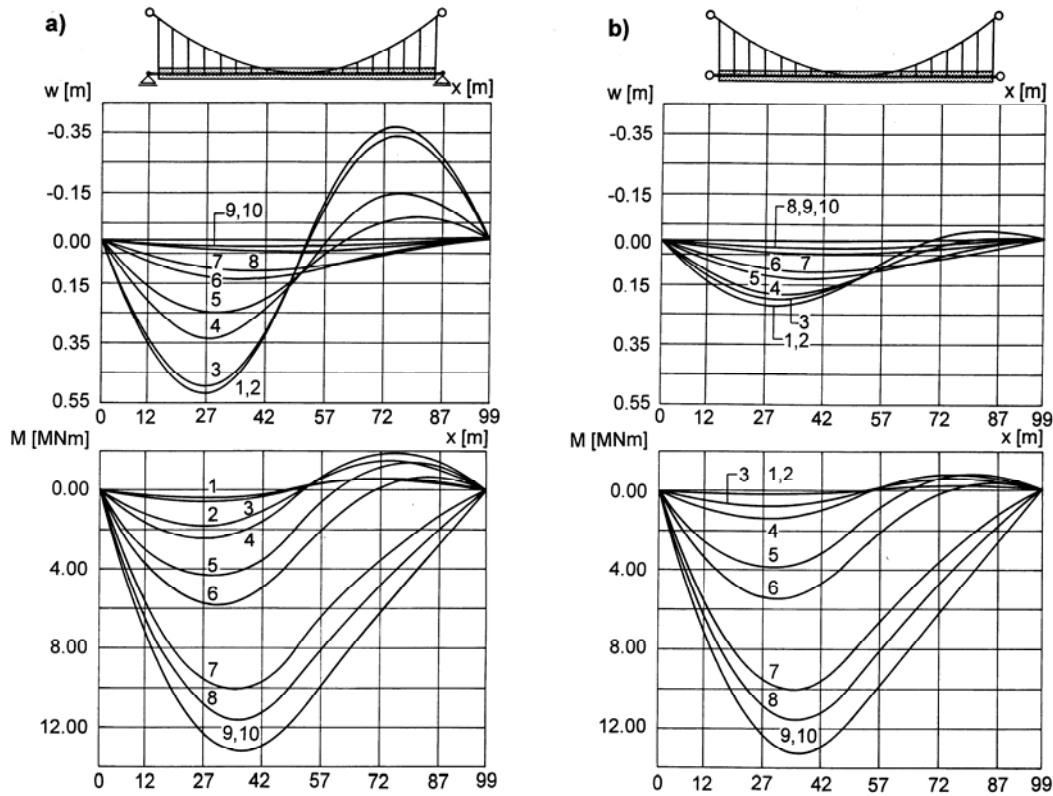


Fig.2.10 – Effects of the live load

It also evident that the bending stresses in slender structures are very low and originate only close to the end anchor blocks. Along the whole length, the structure is stressed by normal forces only.

A similar analysis was performed for the suspension (see Fig.2.10) and cable stayed structures (see Fig.2.11). The deck was supported on movable bearings and connected to the abutments with horizontal springs of stiffness k . Figs.2.10a and 2.11a present results for the $k = 0$, Figs.2.10b and 2.11b presents results for the $k = \infty$.

The suspension structure is formed by a suspension cable of span $L = 99.00$ m and sag $f = 0.1L = 9.90$ m on which a concrete deck is suspended. The total area of the cables is $A_s = 0.00862$ m² and modulus of elasticity is $E_s = 195,000$ MPa. It is assumed that the suspenders are pin connected stiff bars. At the mid-span the suspension cable is connected to the deck.

The deck has the same material and sectional characteristics as the deck in the previous example. Since the deck has a constant area, the dead load $g = 31.25$ kN/m² is also constant. The initial stresses in the suspension cables are derived from the horizontal force:

$$H_g = \frac{gL^2}{8f} = \frac{33.35 \times 99.00^2}{8 \times 1.98} = 20,635 \text{ kN}.$$

The Fig 2.10 shows the deformation $w(x)$ and bending moments $M(x)$ along the length of the bridge for loading by dead load and live load $p = 20.00$ kN/m situated on only one half of the structure. From the figures it is evident how deformation and bending moments depend on the stiffness of the deck and boundary conditions. It is clear that the deformation and bending moment in the deck can be significantly reduced by restraining the horizontal movement of the deck.

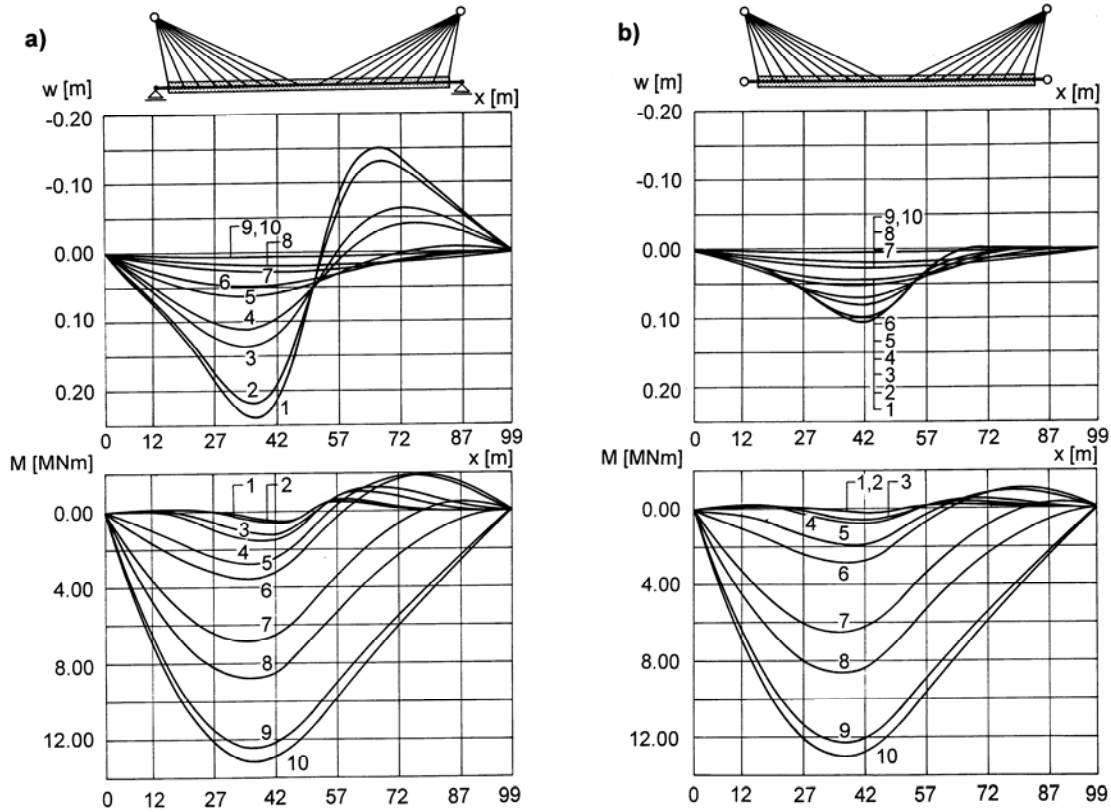


Fig.2.11 – Effects of the live load

Similar results were obtained from the analysis of the cable stayed structure (see Fig.2.11). This structure was also analysed as a 2D geometrically non-linear structure with program *ANSYS*. The initial forces in the stay cables were determined in such a way that they exactly balanced the dead load. The horizontal springs were connected to the deck after the erection.

Books describing the cable stayed structure usually demonstrate their superior behaviour. Fig.2.12 shows the relative deformation of the suspension bridge (a), cable stayed bridge with twin towers (b) and cable stayed bridge with A-towers (c) [7]. The relative deformations are caused by a live load applied in a chess board pattern. From the results it is evident that the higher stiffness of the cable stayed structure together with the A-towers' eliminating the out-of-plane deflections of the legs, enhance the resistance of the system to torsional oscillation.

The reduction of the deflection of the deck for the same loading can also be achieved by eliminating of the horizontal movement of the deck. Fig. 2.13a shows the vertical deformations of the deck of the central span of the Willamette River Bridge [27] for a loading situated on one half of the main span and for different values of the horizontal springs representing the flexible connection of the deck. Similar reduction of deflections and corresponding stresses occurs for loads situated in the main span in a chess board pattern that causes maximum distortions of the deck – see Fig.2.13b.

Eliminating the horizontal movement of the deck generates tension stresses in the deck. In slender structures tension stresses stabilize the structures and reduce the deflections and corresponding bending stresses. This phenomenon is utilized in the prevailing portion of the described structures.

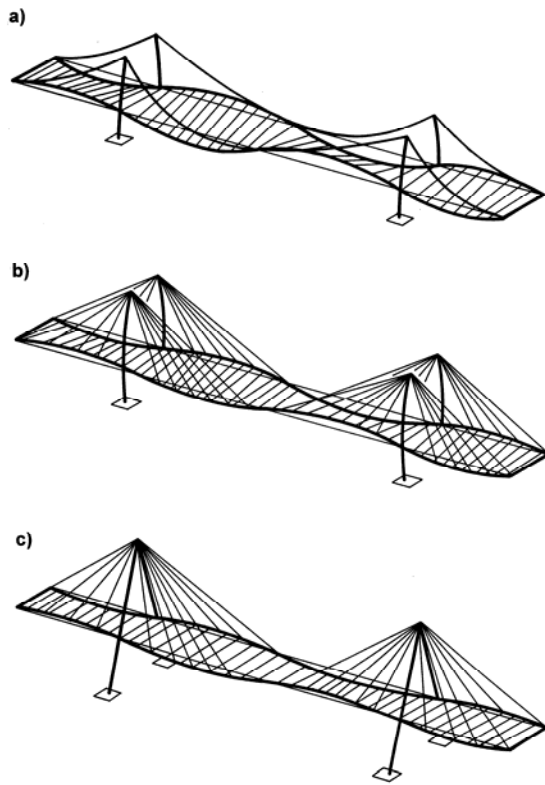


Fig.2.12 – Relative deformations

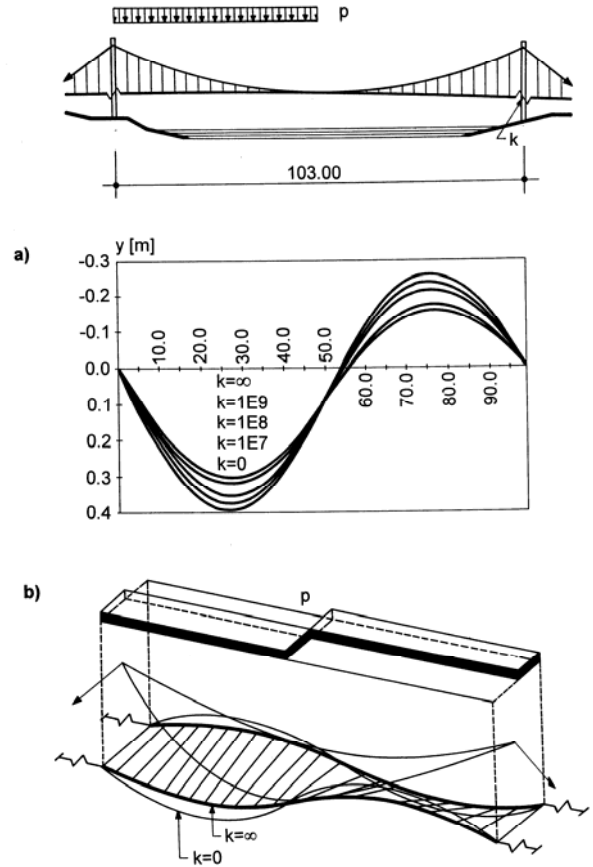


Fig.2.13 – Deformation of the suspension structure

3 CABLE ANALYSIS

Analysis of the stress ribbon and cable supported structures is based on an understanding of the static and dynamic behaviour of a single cable.

In analysis we suppose that a cable of area A and modulus of elasticity E acts as a perfectly flexible member that is able to resist the normal force only. Under this assumption the cable curve will coincide with the funicular curve of the load applied to the cable and to the chosen value of the horizontal force H .

The cable that for the load $q(x)_0$ is stressed by a horizontal force H_0 is for the load $q(x)_i$ stressed by a horizontal force H_i . This force can be easily determined by solving of a cubic equation:

$$aH_i^3 + bH_i^2 + cH_i + d = 0 \quad (3.1)$$

where Ln_i is a nontension length of the cable, k is an elastic deformation of the cable in anchor blocks and

$$a = \frac{l_i}{EA \cos^2 \beta_i} + k, \quad b = Ln_i - \frac{l_i}{\cos \beta_i}, \quad c = \frac{D_i}{EA}, \quad d = \frac{\cos \beta_i}{2} D_i$$

In flexibly supported cables the members a , b , c , d depend on the span l_i and vertical difference h_i which again depend on horizontal force H_i , it is not possible to determine the unknown H_i directly

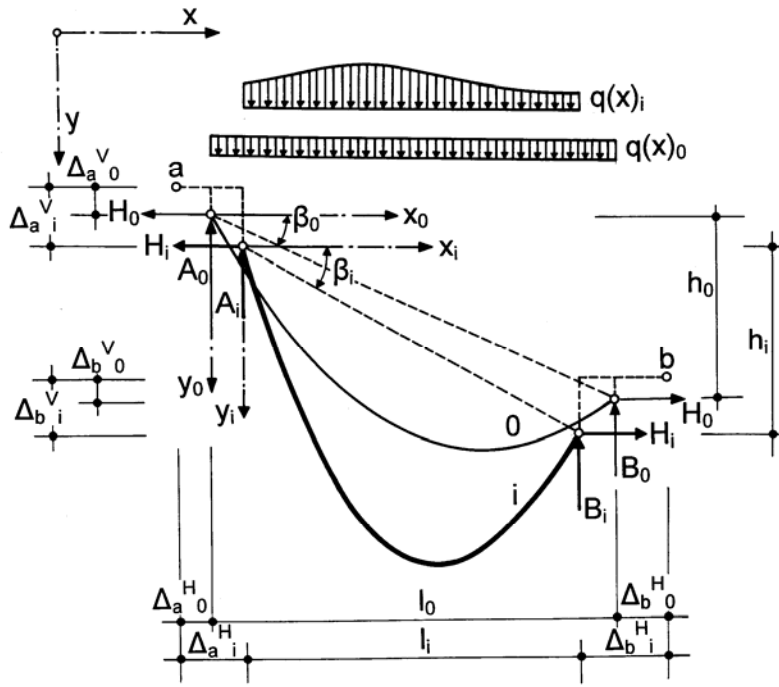


Fig.3.1 Single cable

by solving of the equation. Therefore it is necessary to determine H_i by iteration. First, the unknown H_i is determined for zero deformation of supports and zero elongation of the cable at the anchor blocks. For this force the vertical reactions A_i and B_i , span length l_i and vertical difference h_i and members a, b, c, d and new horizontal force H_i are computed. The computation is repeated till the difference between the subsequent solutions is smaller than the required accuracy.

The bending of the cable is derived from the analysis of a single cable which is stressed by the known horizontal force H [3].

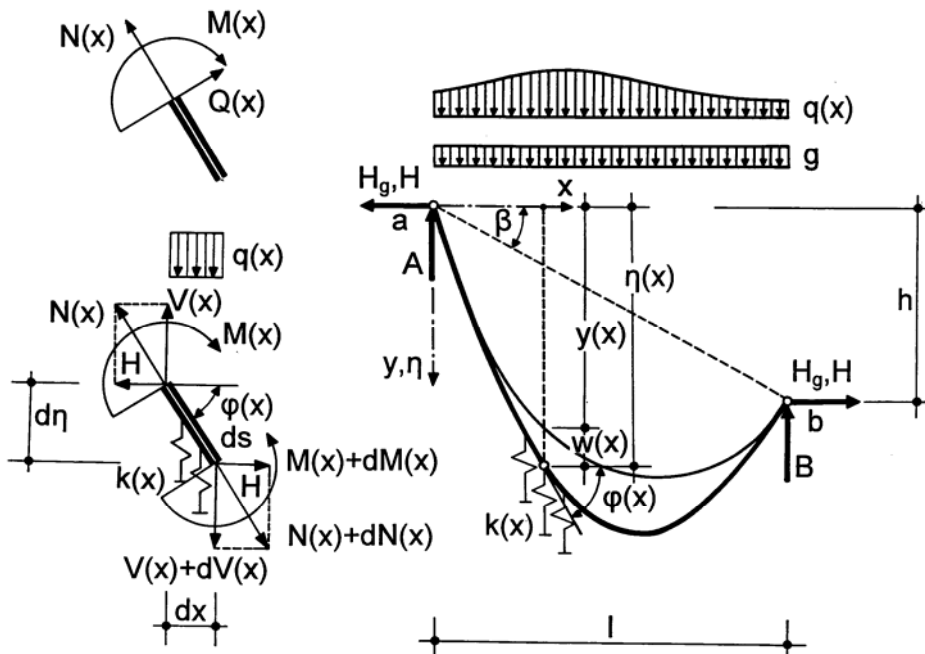


Fig.3.2 Bending of the single cable

The bending moments $M(x) = -EI \frac{d^2 w(x)}{dx^2}$

in the single cable of the area A , moment of inertia I and modulus of elasticity E that is fixed into the supports a and b are determined by solving the equation:

$$EI \frac{d^4 w(x)}{dx^4} - H \frac{d^2 w(x)}{dx^2} + k w(x) = q(x) + \frac{H}{R_g} = q(x) - \frac{H}{H_g} g \quad (3.2)$$

Where load $g(x)$ and horizontal force H_g correspond to the stage without bending and $q(x)$ and H correspond to the analysed stage.

Direct solution of (3.2) is possible only for special cases. For example, the course of the bending moment $M(x)$ in the vicinity of the support of a cable that is loaded by uniform loads g and q and the corresponding horizontal forces are H_g and H is solved for an infinitely long cable – see Fig.3.3a. The bending moment at the infinitely long cable that is loaded by point load F and by uniform load q (see Fig.3.3b) can be derive similarly.

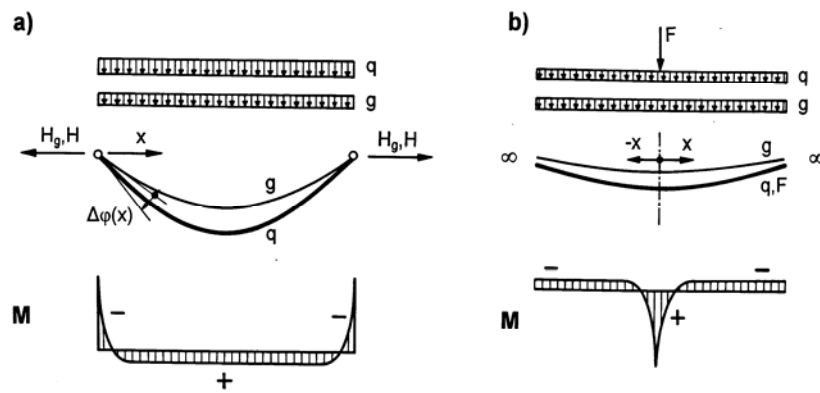


Fig.3.3 Bending of the single cable

$$\lambda = \sqrt{\frac{H}{EI}}$$

$$M(x) = \Delta\varphi \sqrt{H \cdot EI} \cdot e^{-\lambda x} + \Delta q EI$$

$$M(x) = \frac{F}{2\lambda} e^{-\lambda x} + EI \Delta q$$

$$\Delta q = \frac{q}{H} - \frac{g}{H_g}$$

The author, rather than solving the equations for different loading conditions, developed a program in which the deformation and corresponding shear forces and bending moments were solved using *finite difference method* [20],[30]. This approach enables to express a local stiffening of the cable and a supporting of part of the cable by Winkler springs.

In the analysis the cable was divided into short elements of length h (in the actual structure a cable of the length of 100 m was divided into 10,000 elements of a length of 0.010m). The elements can have different stiffness given by EI and can be supported by springs of different stiffness.

To realize the difference between the behaviour of the beam and cable, a stress ribbon and beam structure of spans $L = 33.00, 66.00$ and 99.00 m loaded by uniform load and by vertical deflection of supports are presented here. The stress ribbon was modelled as a cable and analysed by the above process.

The structure have an area $A = 1.25 \text{ m}^2$, moment of inertia $I = 0.0065104 \text{ m}^4$, and modulus of elasticity $E = 36,000 \text{ MPa}$. The stress ribbon structures have sag at midspan $f_{L/2} = 0.02 L$, corresponding horizontal force $H_g = gL^2/8f_{L/2} = 6.25(g.L) = 195.3125 L$. The dead load $g = 31.25 \text{ kN/m}$ does not cause the bending of the structure.

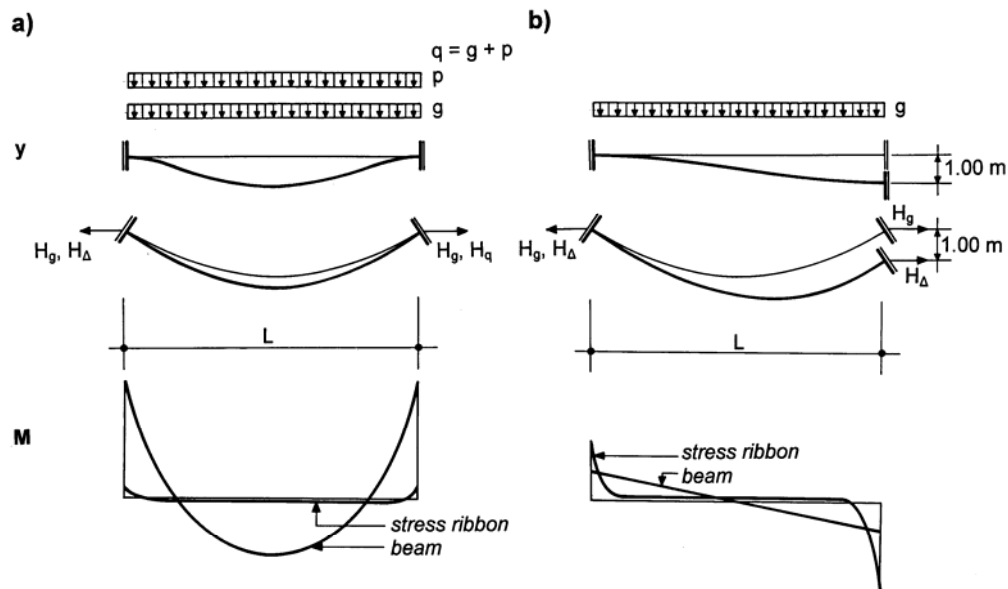


Fig.3.4 Deformation and bending moments at beam and stress ribbon

The Fig.3.4a and Table 3.1 show the deflection and bending moment in the beam and cable for load $p = 20.00$ kN/m. It is evident that the deflections and bending moments in the stress ribbon are very low. The Fig.3.4b and Table 3.2 show the deflection and bending moment in the beam and stress ribbon stressed by a vertical deflection of support $\Delta = 1.00$ m. With an increasing span length the bending moments in the beams are reduced proportionally to the square of their length. On the contrary, the bending moments in the stress ribbon have significant values that in the longer spans are even higher than in the beam. Therefore it is necessary to carefully analyze the bending of cables (or prestressed bands) in structures where significant vertical deformations can occur – for example in cables of a cable supported structure.

Tab.3.1			L [m]		
			33	66	99
M_p	beam	[MNm]	-1.815	-7.262	-16.335
$M_{L/2}$	beam	[MNm]	0.908	3.631	8.168
$y_{L/2}$	beam	[m]	0.527	8.433	42.6933
M_p	stress ribbon	[MNm]	-0.106	-0.339	-0.594
$M_{L/2}$	stress ribbon	[MNm]	0.034	0.039	0.036
$y_{L/2}$	stress ribbon	[m]	0.0115	0.0726	0.1679

Tab.3.2			L [m]		
			33	66	99
$M_{p,a}$	beam	[MNm]	-1.291	-0.323	-0.143
$M_{p,b}$	beam	[MNm]	1.291	0.323	0.143
$M_{p,a}$	stress ribbon	[MNm]	-1.429	-0.787	-0.637
$M_{p,b}$	stress ribbon	[MNm]	2.485	1.166	0.839

4 STRESS RIBBON STRUCTURES

4.1 STRUCTURAL ARRANGEMENT

Stress ribbon bridges can have one or more spans. A lightly draped shape characterizes this structural type. The exact shape of the stress ribbon structure is the funicular line of the dead load. Since these structures usually have a constant cross section and the sag is very small, they have the shape of the second degree parabola.

Only in special cases is the deck cast in formwork supported by a falsework. Usually, the stress ribbon structures are erected independently from the existing terrain. The formwork or precast segments is suspended on bearing tendons and shifted along them into their design position – see Fig.4.1.1a. Prestressing applied after the casting of the whole band, or the joints between the segments, guarantees the structural integrity of the complete deck.

The structural arrangement of stress ribbon bridges is determined by their static function and by their process of construction. During erection, the structure acts as a perfectly flexible cable (see Fig.4.1.1a); during service as a prestressed band (stress ribbon) that is stressed not only by normal forces but also by bending moments (see Fig.4.1.1b). However, the shape and the stresses in the structure at the end of the erection determines the magnitude of the stresses that will occur in the structure during service.

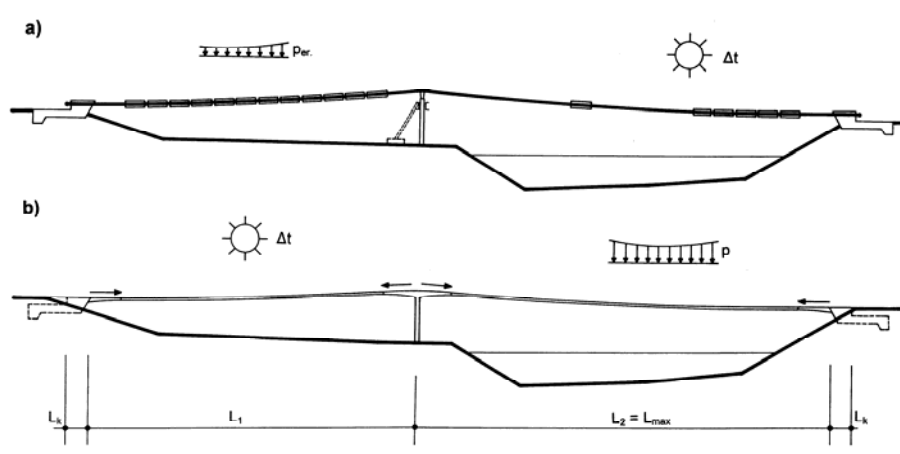


Fig.4.1.1 Static function

It was shown that significant bending moments in the stress ribbon structures originate only at the supports. Since along the whole length of the structure the deck is stressed only by normal forces, the deck can be formed with a very slender solid section that can be further reduced by *waffles* that create a coffered soffit. The minimum area of the deck is determined from the requirement that under the various loading condition (including prestress) there are limited or zero tension stresses in the deck, and that maximum compressive stresses are not exceeded. Since the bending moments due to the point load are low, the depth of the deck is essentially determined by the cover requirements of the prestressing steel. Usually the minimum depth guarantees a sufficient stiffness of the deck.

The typical section of a stress-ribbon is not able to resist the bending moments that occur at the supports. The support bending moments can be reduced by:

- Creating a flexible support member close to the supports – see Fig.4.1.2b. The function of this member is similar to the function of the neoprene rings usually designed for stay cables.
- Supporting the stress ribbon with a saddle from which the band can lift during post-tensioning and temperature drop, and to which the band can return for a temperature increase—see Fig.4.1.2c.

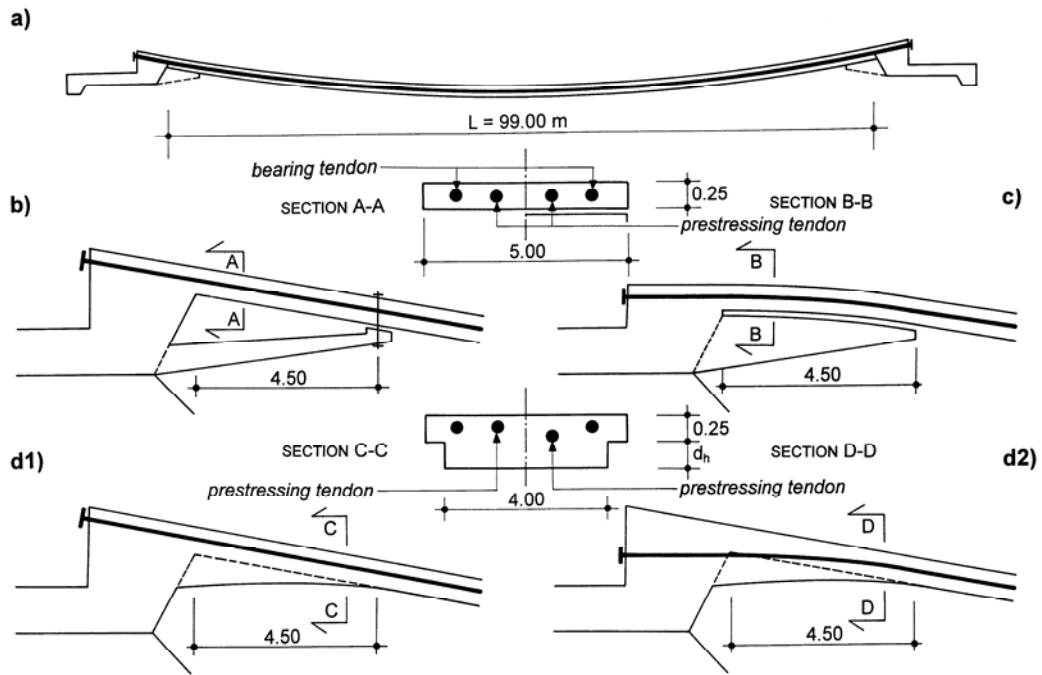


Fig.4.1.2 Stress ribbon at support

Strengthening the stress ribbon with a short support haunch – see Figs.4.1.2.d.

To understand this problem and to quantify the above measures, extensive parametric studies were done. The structure in the Fig.4.1.2d was analyzed for the different arrangements of the stress ribbon close to the supports. The analysis was done for all typical loadings, however only results for the effects of the dead load and prestress are presented in Figs.4.1.3 and 4.1.5.

Fig.4.1.3 shows the bending moments in the stress ribbon near the support for different stiffness of the supporting member. The supporting member was modelled as a beam member of length $l = 1.00$ m and area $A = 1.00$ m², for which the modulus of elasticity E was varied. The stiffness k is a force that causes a deformation $\Delta l = 1$. The analysis was done for $k = 0, 1E+3, 1E+4, 1E+5$ and $1E+6$ kN/m. Fig.4.1.3a presents the analysis results in which the supporting member was attached to the structure before post-tensioning. Fig.4.1.3b presents the results of the analysis where the supporting member was attached after the post-tensioning.

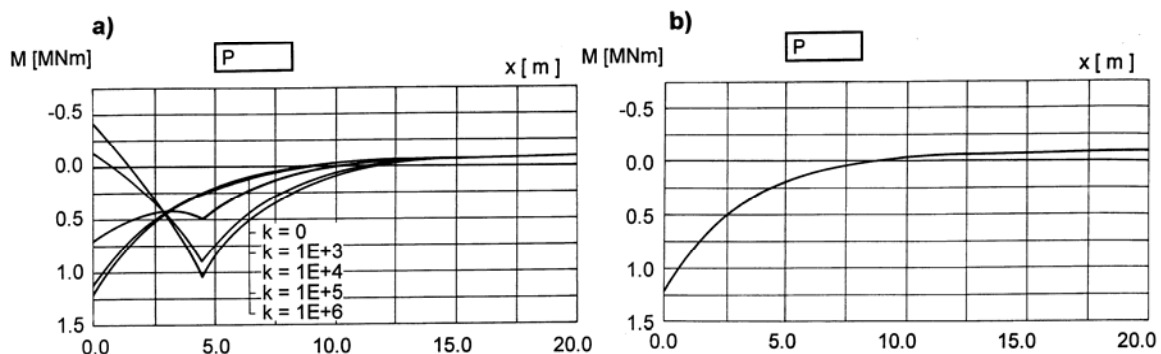


Fig.4.1.3 Bending moments in a structure with flexible supporting member

Fig.4.1.4 shows the bending moments and deformations of the stress ribbon that is supported by a saddle. The surface of the saddle has the shape of a second degree parabola whose tangent at the end of the saddle matches that of the stress ribbon. It was assumed that the saddle is very stiff. Therefore the saddle was modelled by rigid members that were connected to the stress ribbon by

contact members. Since these members do not resist the tension, the ribbon can lift up. Due to the post-tensioning the stress ribbon partially rises from the saddle. It is interesting to note that the stress ribbon never returns to the original position when it is loaded with temperature rise – see Fig.4.1.4b.

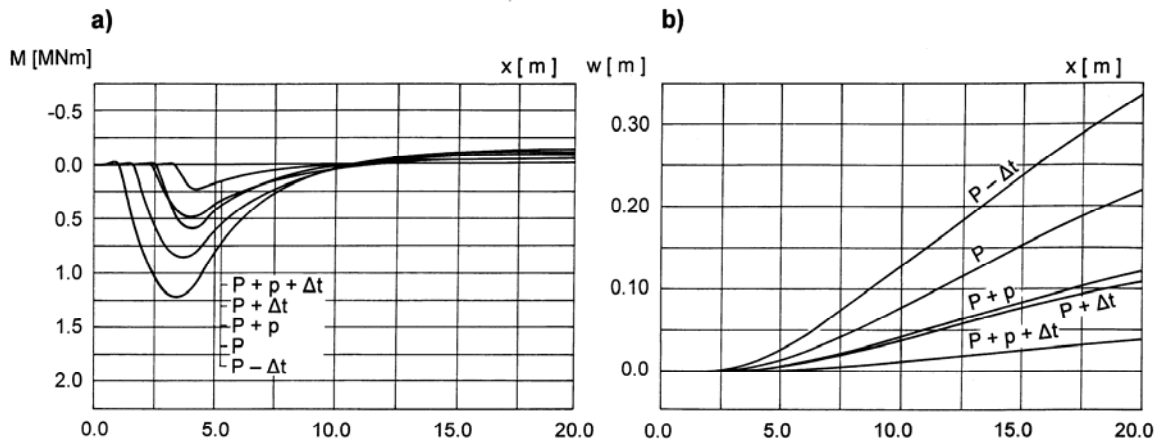


Fig.4.1.4 Bending moments (a) and deformations (b) in a structure with saddle

Fig.4.5 shows the bending moments that occur in the stress ribbon when stiffened by short parabolic haunches. The haunches have a constant width of 4.00 m and variable depth d . The calculations were done at depths $d_h = 0, 0.25, 0.50, 0.75, 1.00$ m. Fig.4.1.5a presents the results for a structure in which prestressing tendons are parallel to the surface of the deck, the Fig.4.1.5b presents the results for a structure in which prestressing tendons follow the centroid of the haunch.

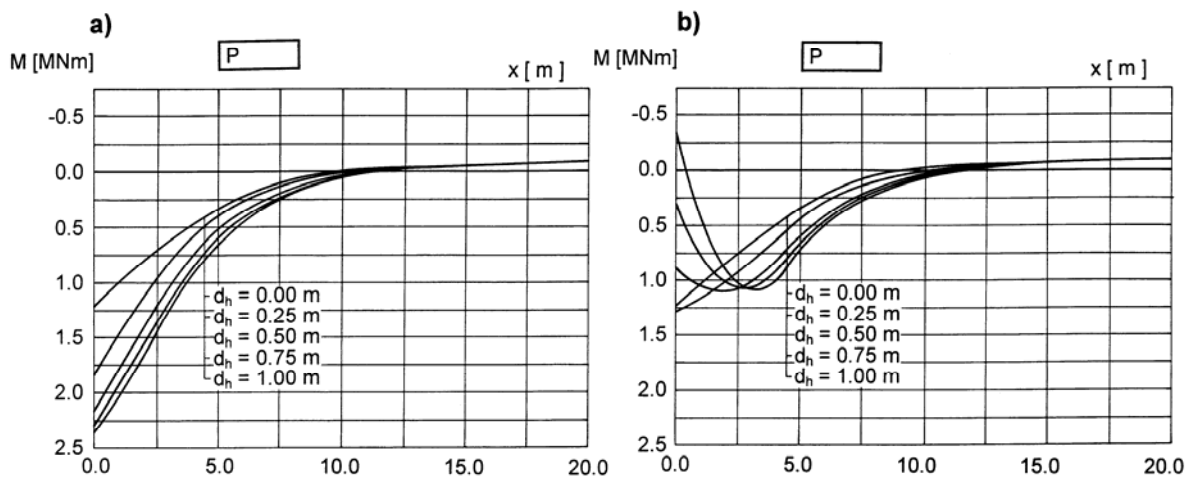


Fig.4.1.5 Bending moments in a structure with haunches

Although the described measures can significantly reduce the bending stresses, it is necessary to carefully design the stress ribbon in the vicinity of the supports. For designing the ribbon, the positive bending moments that cause tension stresses at bottom fibres are critical. Since the bearing and prestressing tendons are situated in a sufficient distance away from the bottom fibres, it is possible to accept cracks there and design the ribbon as a partially post-tensioned member in which crack width and fatigue stresses in the reinforcement are checked. If the ribbon above the saddle is assembled from precast members, it is necessary to guarantee compression in the joints. This can be provided with additional short tendons situated in the pier segments.

4.2 STATIC FUNCTION

As was previously stated, the static behaviour of the stress ribbon structures is given by their structural arrangement and by the process of construction.

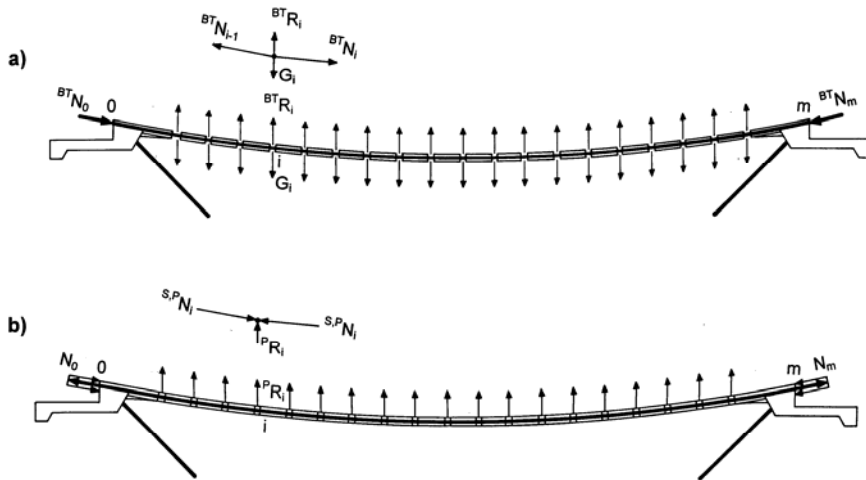


Fig.4.2.1 Precast stress ribbon structure

Figs.4.2.1 and 4.2.2 show a structure that was erected from precast segments (PS) with cast-in place composite slab (CS) slab. The segments of length $l_s = l_p$ were suspended on bearing tendons (BT). After casting the composite slab and joints the structure was post-tensioned with prestressing tendons (PT). The precast segments have an area A_{PC} , composite slab A_{CS} , the bearing tendons A_{BT} and the prestressing tendons A_{PT} . While the modulus of elasticity of the precast segments E_{PC} and the composite slab E_{CS} depend on their age, the modulus of elasticity of the tendons E_s is constant. The weight g is composed of the weight of the bearing and prestressing tendons Tg and the weight of the segments and cast-in-place slab Sg .

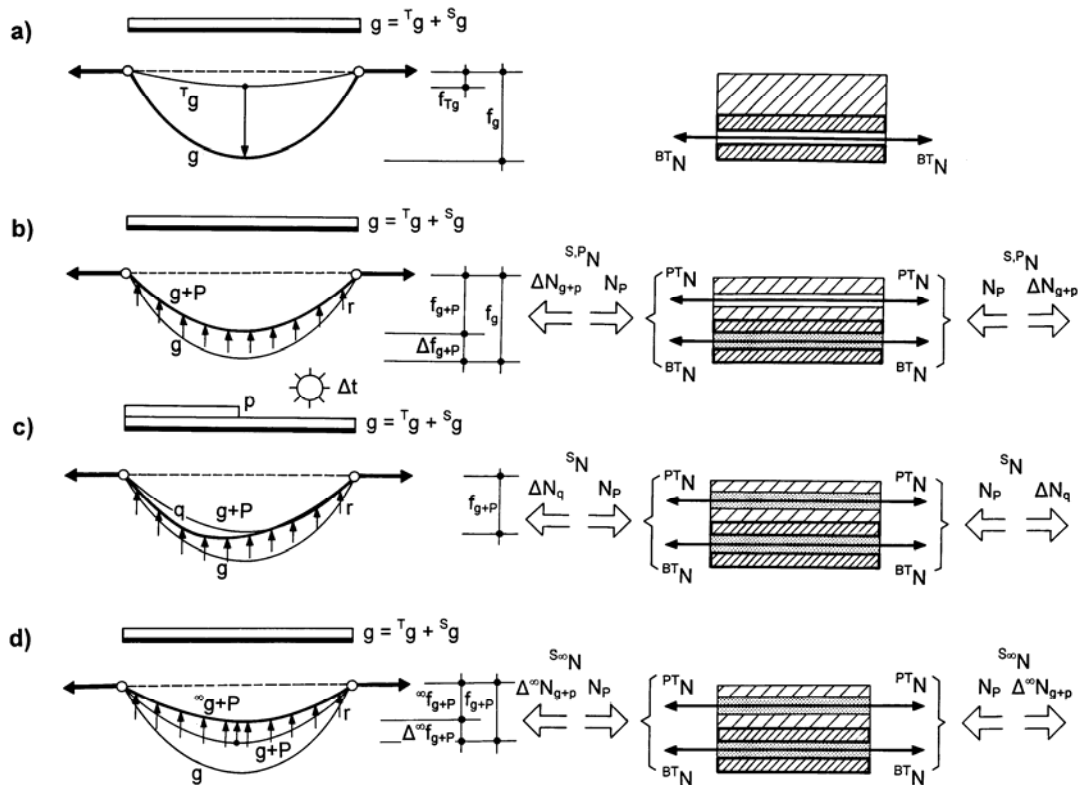


Fig.4.2.2 Loading, deformation and stresses of precast stress ribbon structure

It is interesting to follow the history of the forces that occur in the structure during the construction and during service. After casting the composite slab and joints, the bearing tendons carry all the dead load. They are stressed by a tension force ${}^{BT}N = N_g$. At each joint i , the resultant internal force ${}^{BT}R_i$ in the bearing tendons balances the vertical load $G_i = g l_s$ – see Figs.4.2.1a and 4.2.2a. The anchor blocks are loaded by tension forces ${}^{BT}N_0$ and ${}^{BT}N_m$.

When the concrete in the joints reaches a sufficient strength, the deck is prestressed – see Figs.4.2.1b and 4.2.2b. The structure has now become one continuous structural member with a composite section of modulus or elasticity E_{PC} and effective area ${}^P A_e$.

$${}^P A_e = A_{PC} + \frac{E_{CS}}{E_{PS}} A_{CS} + \frac{E_S}{E_{PS}} A_{BT}$$

By stressing of the prestressing tendons radial forces in the joints ${}^P R_i$ are created. The stress ribbon moves up as a consequence. Since the sag f_g has been reduced to f_{g+p} , the composite stress ribbon consisting of by precast segments (PS), composite slab (CS) and bearing tendons (BT), is stressed not only by compression forces N_p , but also by tension forces ΔN_{g+p} that correspond the sag reduction Δf_{g+p} .

$$\Delta N_{g+p} = N_{g+p} - N_g$$

$$\Delta f_{g+p} = f_{g+p} - f_g$$

The normal force ${}^{S,P}N = -N_p + \Delta N_{g+p}$ is distributed to the precast segments (PS), composite slab (CS) and bearing tendons (BT), in proportion to the modulus of elasticity and area of components. The anchor blocks are loaded by tension forces N_0 and N_m that correspond to the tension of a structure of sag f_{g+p} .

After the prestressing tendons are grouted they become a part of composite section of area A_e and modulus of elasticity E_{PC} .

$$A_e = A_{PC} + \frac{E_{CS}}{E_{PS}} A_{CS} + \frac{E_S}{E_{PS}} A_{BT} + \frac{E_S}{E_{PC}} {}^{PT} A_s$$

All service loads (see Fig.4.2.2c) are resisted by this composite section that is stressed by the normal force

$${}^S N = -N_p + \Delta N_q$$

$$\text{where } \Delta N_q = N_q - N_g$$

N_q is a normal force that originates in the stress ribbon loaded by dead load, live load, temperature changes and by ΔN_{g+p} . ${}^S N$ is distributed proportionally to the modulus of elasticity and area into the precast segments (PS), composite slab (CS), bearing (BT) and prestressing (PT) tendons.

With time, the internal forces in the individual members of the composite section are redistributed because of the creep and shrinkage of concrete. Due to the shortening of concrete the stress ribbon moves up and the original sag f_{g+p} is reduced to ${}^\infty f_{g+p}$. Therefore the stress ribbon is additionally stressed by a tension force

$${}^{S,\infty} N = -N_p + \Delta{}^\infty N_{g+p}$$

$$\text{where } \Delta{}^\infty N_{g+p} = N_{g+p} - N_g - N_{c+sh}$$

where

$$\Delta{}^\infty f_{g+p} = f_{g+p} - f_g - f_{c+sh}$$

${}^{S,\infty} N$ is distributed into all members of the composite section. Also, all service loads now act on a structure that has a reduced sag and therefore higher tension stresses.

It is therefore evident that the stresses in all structural members of the stress ribbon depend on the construction process, age of the concrete members, and time at which the structure is loaded.

It is also clear that it necessary to distinguish between the behaviour of the structure during erection and during the service. During erection the structure acts as a cable (see Fig.4.1.1a), during service as a stress ribbon (see Fig.4.1.1b) that is stressed not only by normal forces but also by bending moments. The shape and the stresses in the structure at the end of erection determine the stresses in the structure when in use. The change from cable to stress ribbon occurs when concrete of the joints starts to set.

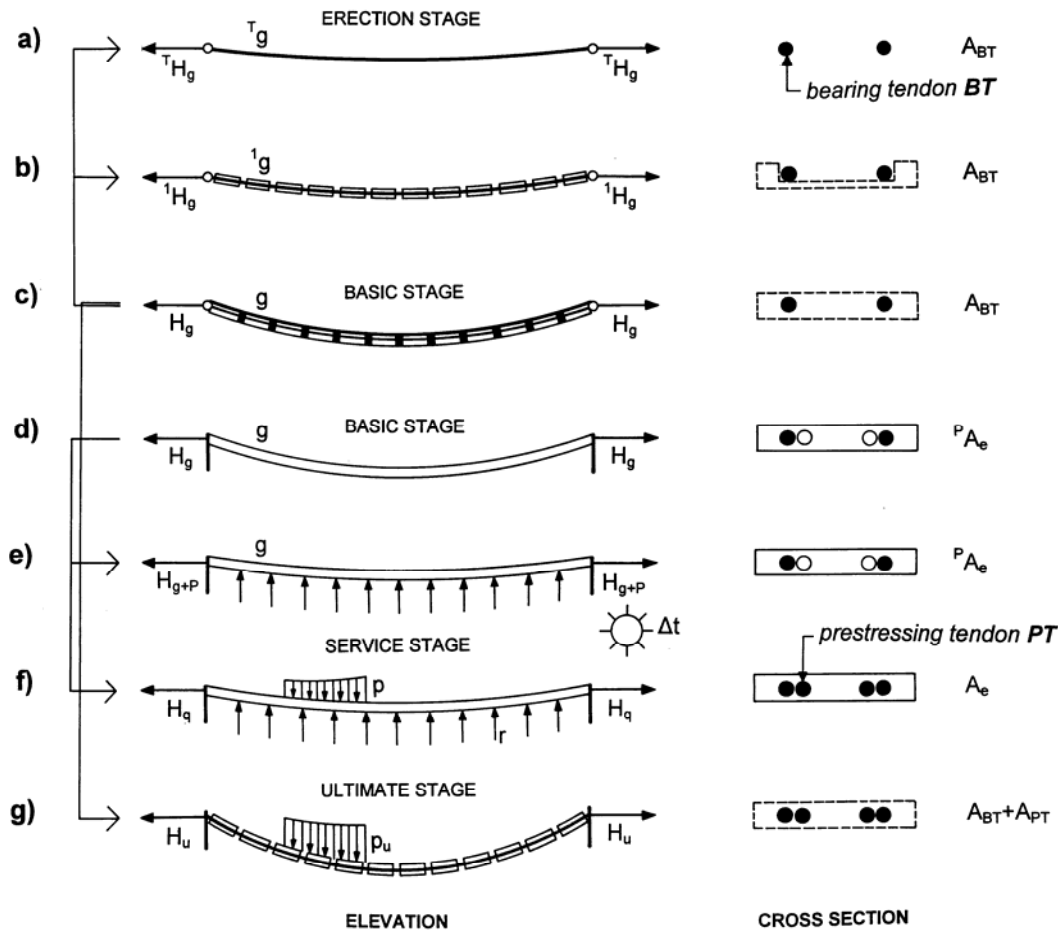


Fig.4.2.3 Loading, deformation and stresses of precast stress ribbon structure

All the design computations have to start from this basic stage. During the erection analysis the structure is progressively unloaded down to the stage in which the bearing tendons are stressed. This is the way the required jacking force is obtained – see Figs.4.2.3a through 4.2.3c. The designer sets the shape of the structure after prestressing – see 4.2.3e. Since this shape depends on the deformation of the structure due to prestress, the basic stage has to be estimated; then the deformation of the structure due to prestress computed and checked against the required final stage. This computation has to be repeated until reasonable agreement is obtained. The basic stage is also the initial stage for the subsequent analysis of the structure for all service loads – see Figs.4.2.3d through 4.2.3f.

4.3 STATIC ANALYSIS

What follows is a description of a simplified analysis that the author used in his first structures. This approach can be used for preliminary analysis or for checking results obtained from modern analytical programs discussed further.

During the erection all loads are resisted by the bearing tendons that act as a cable. Since the tendons are not usually connected to the saddles they can slide freely according to the imposed load. Hence, the cables act as a continuous cable of m spans which crosses fixed supports – see Fig.4.3.1.

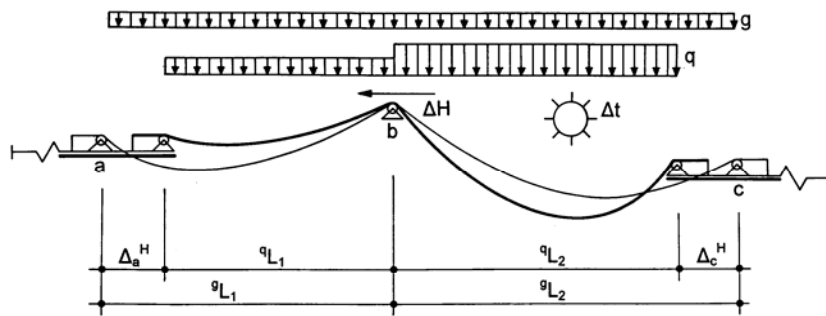


Fig.4.3.1 Stage of erection

Since the stress ribbon structure is very slender, local shear and bending stresses develop only under point loads and at the supports. Because these stresses are relatively small, they do not affect the global behaviour of the structure. This makes it possible to analyze the stress ribbon structure in the final stage as a cable too. The analysis is done in two closely related steps:

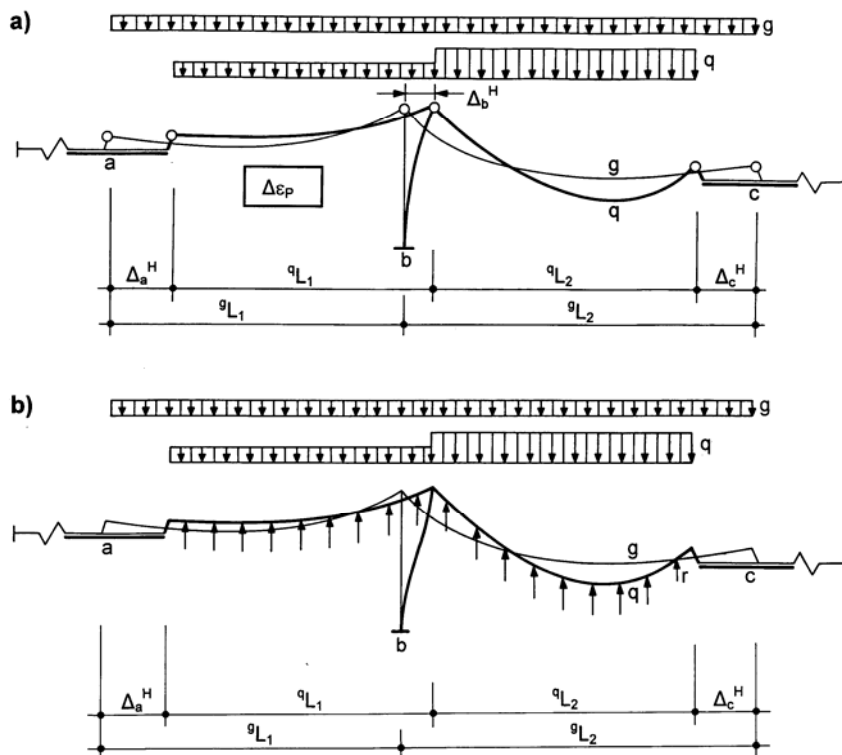


Fig.4.3.2 Stage of service

In step 1, the stress ribbon is analyzed as a perfectly flexible cable which provides the supports – see Fig.4.3.2a. The effect of prestressing is a shortening of the cable, which can be simulated as a temperature drop. The effect of creep and shrinkage can be analysed in a similar way. However, due to the redistribution of stresses between the individual components of the concrete section, an iterative approach has to be used. To facilitate this analysis, standard computer programs for

continuous cables are used. It is also possible to isolate and analyse the individual spans for the given loads and for different horizontal support movements. From the requirement that horizontal force be the same at each span, the horizontal force (H_i) is obtained. With this, the deformations of the supports of the single spans can be calculated.

In step 2, shear and bending stresses in single spans are calculated using the analysis of the bending of the simple cable – see Chapter 3. The cable is analyzed for the load $q(x)$, and for the horizontal force and deformations of the supports that were determined in step 1.

Modern structural programs utilizing Newton-Raphson method allow us to follow the behaviour of the stress ribbon structures both during erection and during service –see Fig.4.3.2b. These programs also need to capture the large deformation and the tension stiffening effects. The structure can be modelled as a chain of parallel members that represent bearing tendons (BT), prestressing tendons (PT), precast segments (PS) and cast-in-place slab (CS) or trough – see 4.3.3. Bearing and prestressing tendons can be modelled as ‘cable’ members, for which the initial force or strain has to be determined. Precast segments and cast-in-place slab can be modelled as 3D bars or as shell elements that have both bending and membrane capabilities.

Since the programs use so called ‘frozen members’ it is possible to model a change of the static system (from the cable into the stress ribbon) as well as the progressive erection of the structure.

The program systems also contain so called ‘contact’ members that only resist compression forces. These members can be used for the modeling of saddles from where the stress ribbons can lift up.

In the analysis the initial stress in the tendons has to be determined. The initial forces are usually determined for the basic stage (see Fig.4.2.3c and 4.2.3d) where the structure changes from cable to stress ribbon. The initial forces in the cable are determined using the cable analysis.

The analysis that starts from the basis stage can be used for both the analysis of the erection and service stages. The stresses in the structure during erection and the bearing tendons jacking forces are determined by simulating a progressive unloading of the structure. Since the superposition principle does not apply, the analysis of the service stage should be carried out according to the following flow chart.

PRESTRESSING EFFECTS

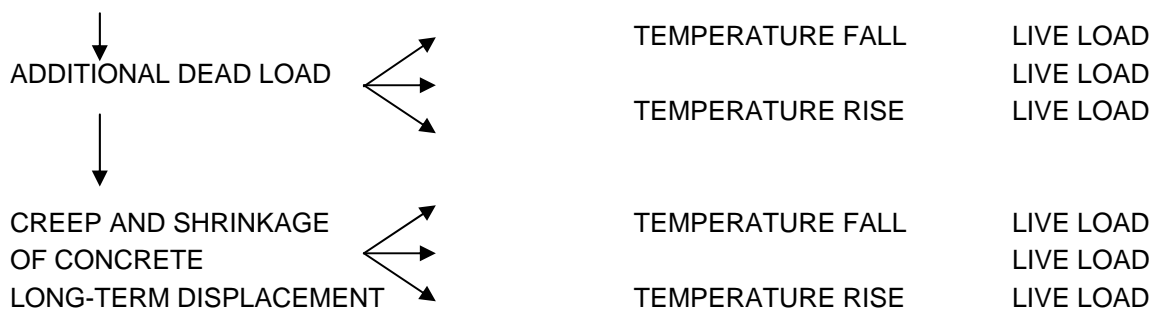


Fig.4.3.3 shows a shape and bending moment (a), and a calculation model (b) of a one span structure loaded by dead load, prestress, and creep and shrinkage of concrete. It is evident that due to creep and shrinkage the sag is reduced and therefore all internal forces are higher at time t_{∞} .

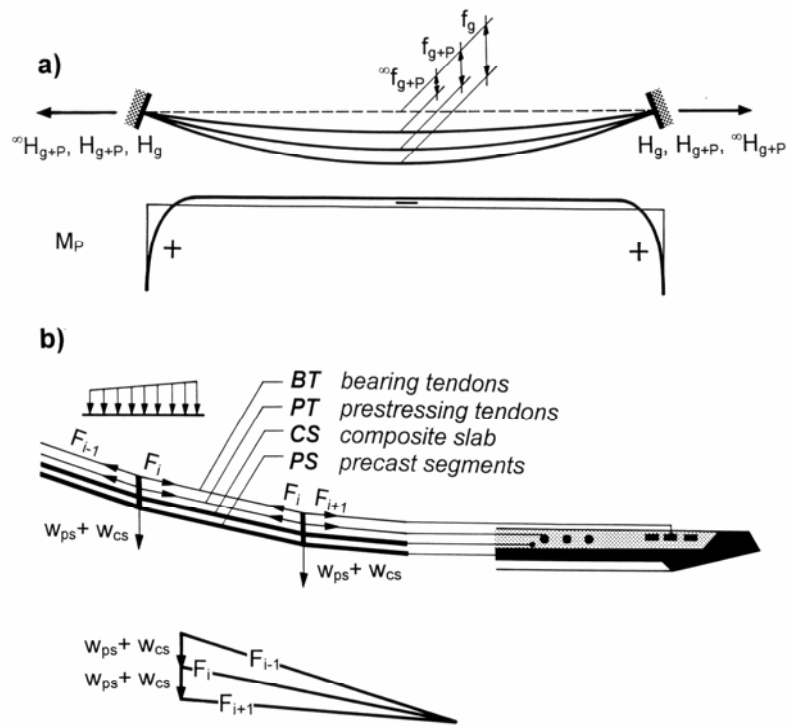


Fig.4.3.3 Deformations and bending moments (a), modelling of the deck (b)

Furthermore, since the area of the bearing and prestressing tendons is higher than in traditional concrete structures, a significant redistribution of stresses between steel and concrete occurs with time. In structures assembled from precast segments and cast-in-place slab the redistribution of stresses between these members also has to be considered.

For the analysis of the creep and shrinkage it is necessary to perform a time dependent analysis. It is not possible to analyse the structure in a single step for the initial strain caused by creep and shrinkage. This would cause significantly larger deformations and higher bending moments at the supports. The author used the procedure combining time-dependent analysis with the finite element software package ANSYS [26].

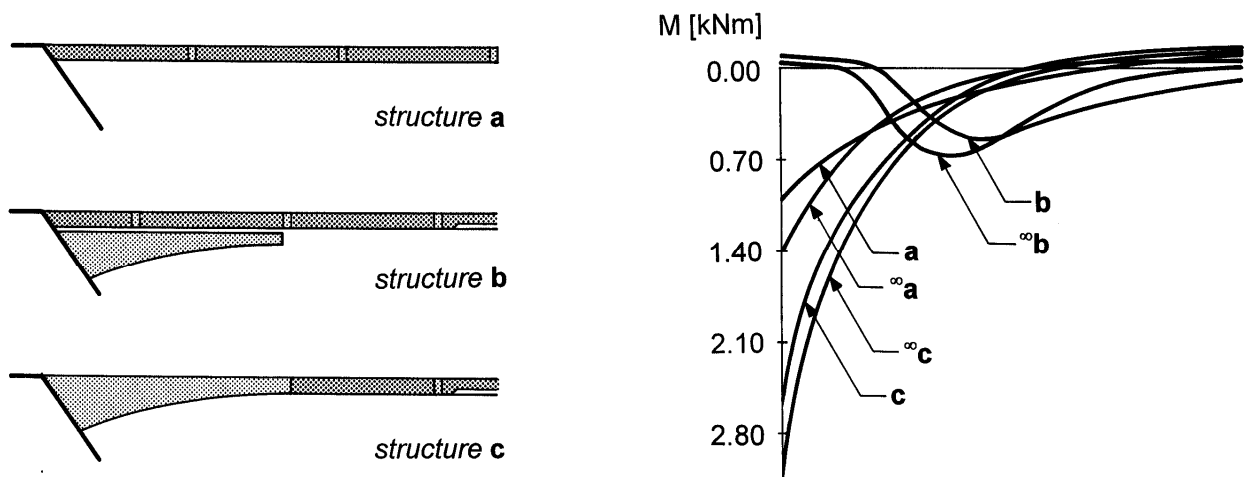


Fig.4.3.4 Bending moments at support

During the design of the Blue River Bridge, Colorado, USA [29] the author carried out a detailed time dependent analysis of the structure. The structure is formed by precast segments with cast-in-place slab. The segments were suspended on bearing tendons and stressed by prestressing tendons. The actual bridge is formed by a stress ribbon that has cast-in-place haunches at supports.

For understanding of the problem the analysis was done for three possible arrangement of the structure: a structure (see Fig. 4.3.4) where the support region was detailed with a constant section (a), with a 4.5 m saddle (b) and with a 4.5 m parabolic haunch (c). The structure was analysed for the effects of prestress and creep and shrinkage of concrete using the CEB-FIP (MC 90) rheological functions.

Figure 4.3.4 shows the bending moments in the stress ribbon close to supports for time t_0 and time t_∞ . Here it can be seen that the bending moments do not change significantly with time.

4.4 DYNAMIC ANALYSIS

The dynamic response of the stress ribbon structures have to be carefully checked for vibration induced by people and wind. Also response to earthquake loading has to be verified. Typically, the first step is to determine the natural modes and frequencies followed by a check of the dynamic response due to the moving load. For preliminary calculations the vertical natural modes can be determined using the formulas for vibration of a simple cable. The dynamic test has proved their validity.

For final design the dynamic analysis should be done with a calculation model that includes non-linear analysis. It is important to realize that the dynamic analysis is usually linear and that most programs are able to describe the special behaviour of the stress ribbon and cable supported structures only by using the so called tension stiffening effect.

A typical one span stress ribbon structure is characterised by natural modes that are presented in Fig.4.4.1. The vertical modes are denoted as A and B; the first swing mode is denoted as C; and the first torsional mode is denoted as D. Due to the vertical curvature of the prestressed band, a horizontal movement is always combined with torsion and it is therefore difficult to find a pure torsional mode. Since the vibration following the first vertical mode (A) requires an elongation

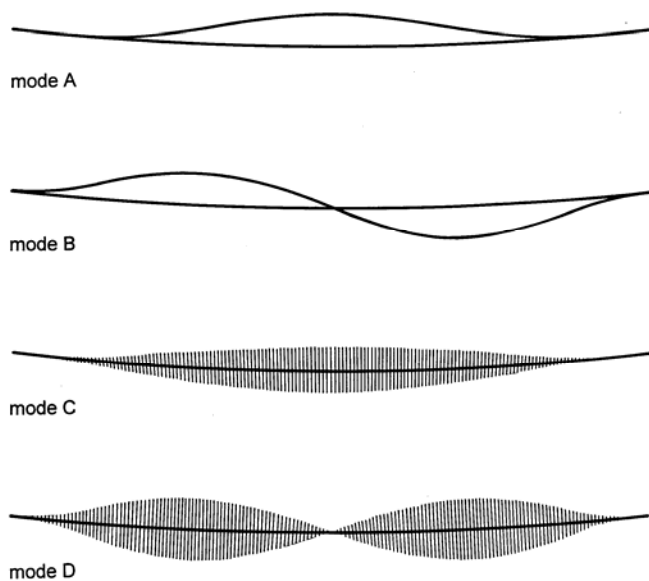


Fig.4.4.1 Natural modes

of the cable, the corresponding frequency is in some cases higher than the frequency of the second vertical mode (B).

When analyzing multi-span structures it is noted that the bridge behaves as a continuous structure only when there is horizontal displacement of the supports. For a small load, as caused by a group of pedestrians, the change of stresses is very small and the individual spans behave as isolated cables. Therefore, when the structure is checked for motions that can cause unpleasant feeling, the dynamic analysis should be done for the individual spans in addition to the overall structure.

4.5 EXAMPLE OF THE ANALYSIS

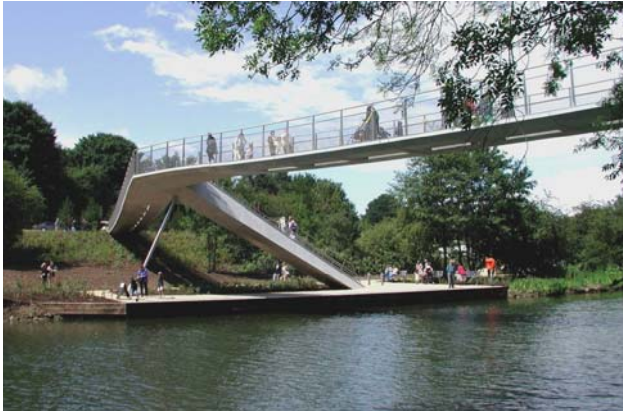


Fig.4.5.1 Maidstone Bridge

For analysis of the stress ribbon bridge built in Maidstone, UK (see Fig.4.5.1) [1] a calculation model presented in Fig.4.5.2 was used. The structures were modelled as 3D structures assembled from parallel 3D elements that modelled precast segments (PS), composite slab (CS), bearing (BT) and prestressing tendons (PT). The length of the elements corresponded to that of the segments.

Fig.4.5.3 presents the bending moment diagrams in the stress ribbon deck of the Maidstone Bridge. Due to the arrangement of the prestressing tendons at the abutments and pier haunches, the positive bending moments that usually appear at those locations were significantly reduced.

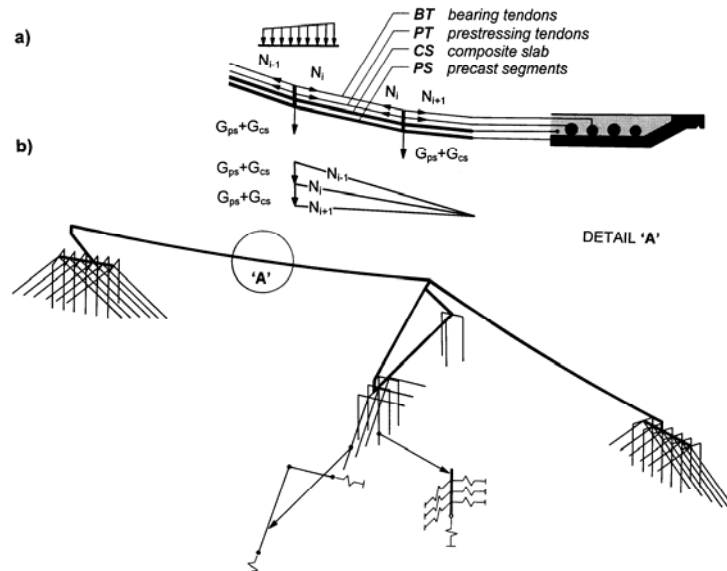


Fig.4.5.2 Calculation model

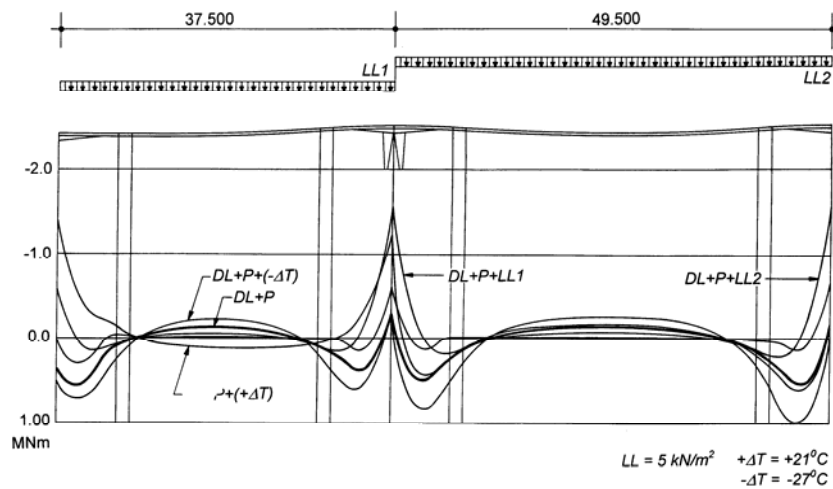


Fig.4.5.3 Bending moments in the deck

4.6 STRESS RIBBON SUPPORTED BY ARCH

The intermediate support of a multi-span stress ribbon can also have a shape of the arch - see Fig.4.6.1. The arch serves as a saddle from which the stress ribbon can rise during post-tensioning and during temperature drop, and where the band can rest during a temperature rise.

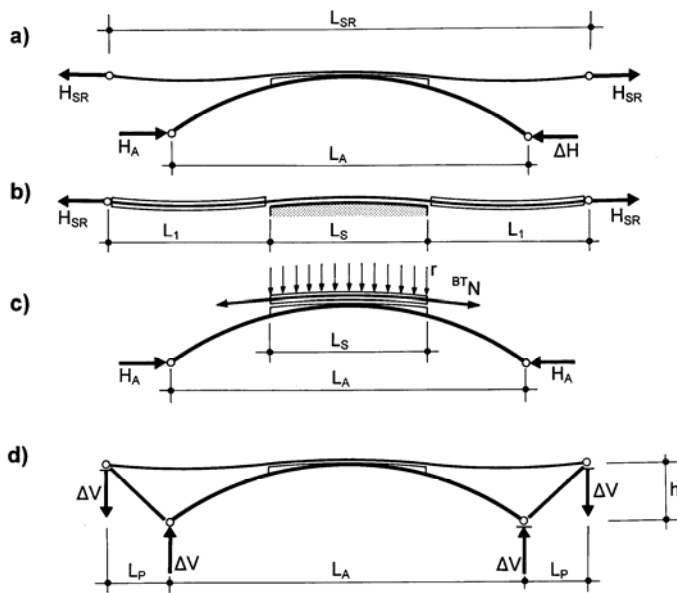


Fig.4.6.1 Stress ribbon supported by arch

In the initial stage the stress ribbon behaves as a two span cable supported by the saddle that is fixed to the end abutments – see Fig.4.6.1b. The arch is loaded by its self weight, the weight of the saddle segments and the radial forces caused by the bearing tendons – see Fig.4.6.1c. After post tensioning the stress ribbon with the prestressing tendons, the stress ribbon and arch behave as one structure.

The shape and initial stresses in the stress ribbon and in the arch can be chosen such that the horizontal forces in the stress ribbon H_{SR} and in the arch H_A are same. It is then possible to connect the stress ribbon and arch footings with compression struts that balance the horizontal forces. The

moment created by horizontal forces $H_{SR}.h$ is then resisted by the $\Delta V.L_P$. In this way a self anchored system with only vertical reactions is created – see Fig.4.6.1d.

The author believes that a structural system formed by a stress ribbon supported by an arch increases the field of application of stress ribbon structures. Several analyses were under taken to verify this. The structures were checked not only with detailed static and dynamic analysis, but also on static and full aeroelastic models. The tests verified the design assumptions, behaviour of the structure under wind loading and determined the ultimate capacity of the structural system.

The model tests were done for a proposed pedestrian bridge across the Radbuza River in Plzen. This structure was designed to combine a steel pipe arch with a span length of 77.00 m and ‘boldness’ of 973 m (ratio of square of the length L divided by the rise f) with a stress-ribbon deck. The behaviour of the structure was confirmed by detailed static and dynamic analysis performed with the program system ANSYS.

The static physical model was done in a 1:10 scale. The shape and test set-up is shown in Fig.4.6.2. Dimensions of the model and cross-section, loads and prestressing forces were

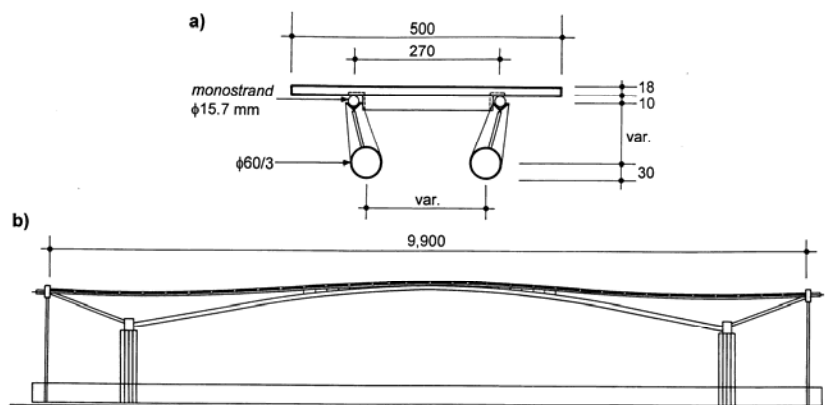


Fig.4.6.2 Static model

determined according to the rules of similarity. The stress ribbon was assembled with precast segments of 18 mm depth and the cast-in-place haunches were anchored in anchor blocks made with steel channel sections. The arch consisted of two steel pipes, and the end struts consisted of two steel boxes fabricated from channel sections. The saddle was made with by two steel angles supported on longitudinal plates strengthened with vertical stiffeners.

The precast segments were made from micro-concrete of 50 MPa characteristic strength. The stress ribbon was supported and post-tensioned by 2 monostrands situated outside the section. Their position was determined by two angles embedded in the segments. These angles were welded to transverse diaphragms situated outside the segments.

The loads, determined according to the rules of similarity, consisted of steel circular bars suspended on the transverse diaphragms and on the arch. The number of bars was modified according to desired load.

The model was tested for the 5 positions of live load. The tested structure was also analysed as a geometrically non-linear structure using the program ANSYS. For all erection stages and for the 5 load cases, the measurement results were compared to that of the analysis. The results presented in [29] demonstrate a reasonable agreement between the analysis and the measurement.



Fig.4.6.3 Ultimate load

At the end of the tests the ultimate capacity of the overall structure was determined. It was clear that the capacity of the structure was not given by the capacity of the stress ribbon since after the opening of the joints the whole load would be resisted by the tension capacity of the monostrands.

Since the capacity of the structure would be given by the buckling strength of the arch, the model was tested for a load situated on one side of the structure – see Fig.4.6.3. The structure was tested for an increased dead load (1.3 G) applied using the additional suspended steel rods, and then for a gradually increasing live load P applied with force control using

a hydraulic jack reacting against a loading frame.

The structure failed by buckling of the arch at a load 1.87 higher that the required ultimate load $Q_u = 1.3 G + 2.2 P$. The stress ribbon itself was damaged only locally by cracks that closed after the load was removed. The structure also proved to be very stiff in the transverse direction.

The buckling capacity of the structure was also calculated with a nonlinear analysis in which the structure was analysed for a gradually increasing load. The failure of the structure was taken at the point when the analytic solution did not converge. Analysis was performed for the arch with and without fabrication imperfections. The imperfections were introduced as a sinus shaped curve with nodes at arch springs and at the crown. Maximum agreement between the analytical solution and the model was achieved for the structure with a maximum value of imperfection of 10 mm. This value is very close the fabrication tolerance.

The test has proven that the analytical model can accurately describe the static function of the structure both at service and at ultimate load. The dynamic behaviour of the proposed structure was also verified by a dynamic and wind tunnel tests performed by Professor Miros Pirner at the Institute of Theoretical and Applied Mechanics, Academy of Sciences of the Czech Republic.

4.7 STATIC AND DYNAMIC LOADING TESTS

The design assumptions and quality of workmanship of the author's first stress ribbon structure built in the Czech Republic [18],[19] and of the first stress ribbon bridge built in United States [14] were checked by measuring the deformations of the superstructure at the time of prestressing and during loading tests. Dynamic tests were also performed on these structures. Only a few key results of a typical structure are given here. Since the shape of a stress ribbon structure is extremely sensitive to temperature change, the temperature of the bridge was carefully recorded at all times.



Fig.4.7.1 Prague-Troja Bridge - load test

The pedestrian bridge in Prague-Troja was tested by 38 vehicles weighing between 2.8 and 8.4 tons – see Fig.4.7.1. First, the vehicles were placed along the entire length of the structure, and then they were placed on each span. During the test only the deformations in the middle of the spans and the horizontal displacements of all supports were measured – see Table 4.7.1. As can be seen, the comparisons are very good.

Table 4.7.1 Prague-Troja Bridge - deflections at midspans

Loaded span		Span 1 mm	Span2 mm	Span3 mm
1,2,3	Calculation	40	200	56
	Measurement	40	186	57
1	Calculation	301	-124	-62
	Measurement	272	-92	-48
2	Calculation	-126	312	-78
	Measurement	-95	289	-50
3	Calculation	-38	-76	221
	Measurement	-25	-56	182

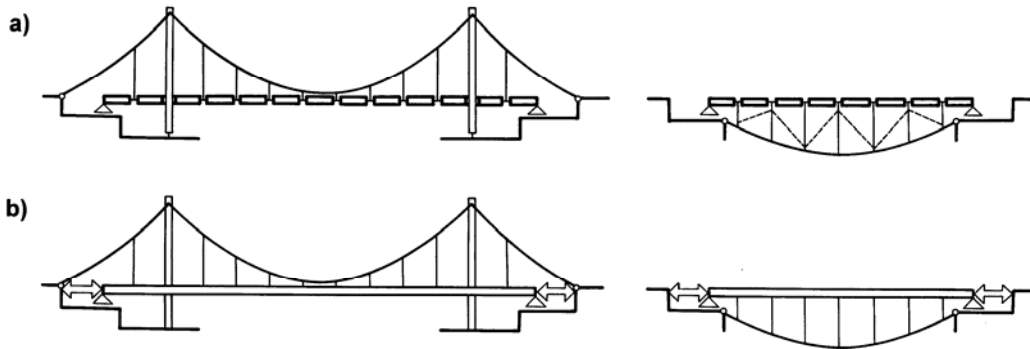
The stress ribbon structures DS-L built in Brno-Bystrc, Brno-Komín, Prerov and Prague-Troja were also subjected to dynamic tests done by Professor Miros Pirner from the Institute of Theoretical and Applied Mechanics, Academy of Sciences of the Czech Republic. In the course of the load tests the agreement of excited natural frequencies with theoretical values was investigated. The structures were excited either by a human force, or by a pulse rocket engine, or by a mechanical rotation exciter [18]. The bridge in Prague-Troja was dynamically tested again after 14 years of service. The second test has proved that the dynamic response of the structure has not changed.

5 SUSPENSION STRUCTURES

Suspension structures are described in many excellent books [5], [15], [31]. Therefore only additional information about suspension structures with slender deck is discussed in this chapter.

5.1 STRUCTURAL ARRANGEMENT

A suspension cable can be anchored into the soil (see Figs.5.1.1) and form a so called earth anchored system; or it can be anchored into the deck and create self anchored systems (see Figs.5.1.2). The suspension cables can be situated above the deck, under the deck or above and under the deck.

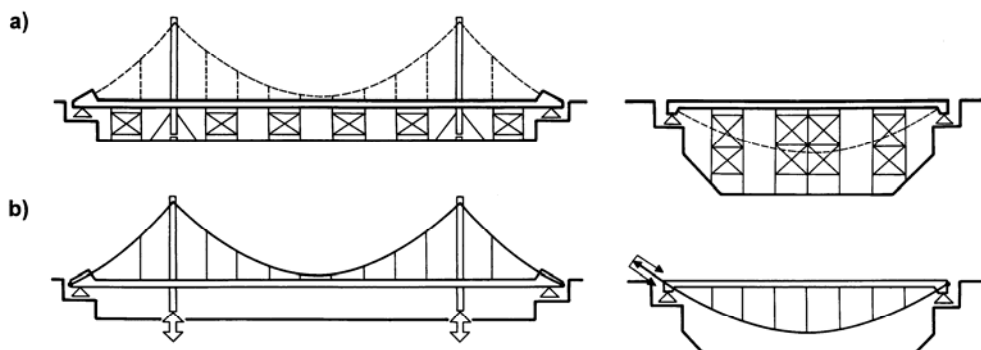


Obr.5.1.1 Earth-anchored suspension structure: a) erection, b) service

The suspension cable has a funicular shape owing to the self-weight of the structure – it balances the effects of the self-weight and guarantees that the structural members are stressed by normal forces only. For service loads the suspension structure forms a complex system in which the deck distributes the load and all structural members contribute to the resistance of the structural system.

The advantage of the earth anchored system is that the erection of the deck can be done independently on the terrain under the bridge. However, the suspension cables have to be erected at first and the anchor blocks have to transfer a large tension force into the soil.

On the other hand the self anchored suspension bridges do not require expensive anchor block and utilize the compression capacity of concrete deck. However, the erection of the deck has to be done at first; then the suspension cables can be erected and tensioned. The fact that the erection of the deck requires a falsework and therefore it depends on the terrain under the bridge banned using this system in many cases.



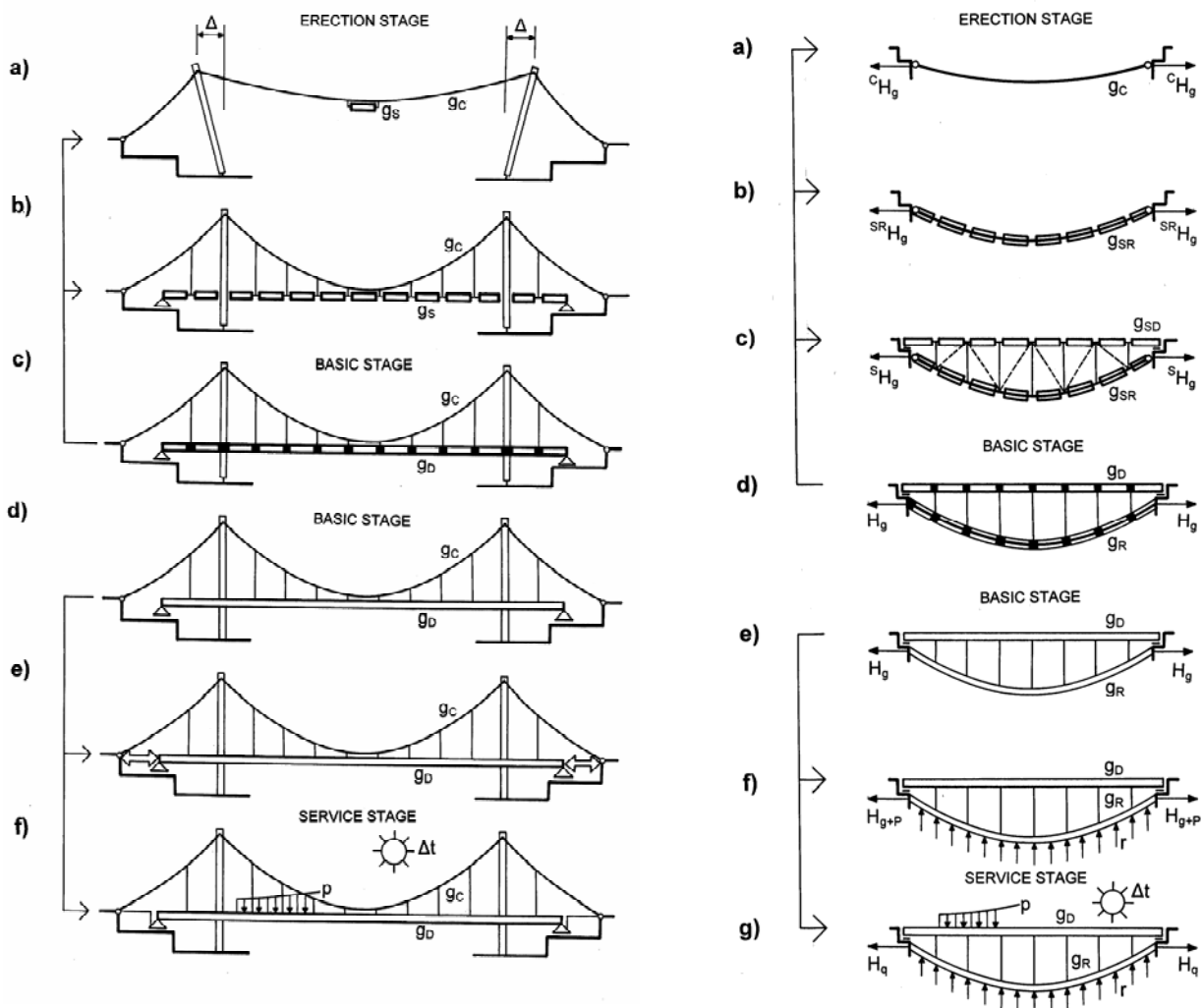
Obr.5.1.2 Earth-anchored suspension structure: a) erection, b) service

In several new applications the erection of the structures is designed in such a way that anchor blocks are designed for erection loading only; when the erection is completed a portion or the whole tension force is transferred from the anchor blocks into the deck. In this way, a partial or total self anchored system is created – see Fig.5.1.1b.

The earth suspension bridges are usually assembled of precast members (segments) that are suspended on suspension cables. Since the precast segments are mutually connected by pins, the suspension cables have automatically a funicular shape owing to the given load. The self anchored structures are usually cast-in-place on the falsework. The self-weight is transferred into the suspension cables by their post-tensioning that can be done by jacking at their anchors or by lifting of the tower. This operation requires careful determining of the camber of the deck and non-tension length of the cables.

5.2 STATIC AND DYNAMIC ANALYSIS

The analysis of the structure both for the erection and service load starts from the initial basic stage. During the erection analysis the structure is progressively unloaded till the stage in which the structure is formed by a cable only (see Fig.5.2.1). Also an initial inclination of the towers is determined.



Obr.5.2.1 Earth-anchored suspension structure: static function

The analysis of the structure for service load also starts from the same initial basic stage. However, after casting and post-tensioning of the joints between the segments, the deck has an actual stiffness and contributes to the resistance of the structure to service load. The analysis of a suspension structures supported by cables is similar. If the structures are supported by a stress ribbon, not only deck and struts are removed, but also the segments forming the ribbon. The analysis of the structure for service load starts by post-tensioning of the stress ribbon.

Analysis of the self anchored structures also starts from the basic stage for which optimum forces in suspension cables were determined. The shape of the structure during the assembly or casting is obtained by unloading the structure by removing of prestressing force in cables. The analysis of the structure for service load is the same as in the earth anchored structure.

For understanding the behaviour of a typical suspension structure of a span $L = 99$ m, extensive parametric studies were done. At first, the influence of the sag, connection of the deck with suspension cables at midspan and restriction of the horizontal movement at support were studied on a 2D suspension structure. Then the space behaviour of a 3D suspension structure was analysed.

The structure of the span $L = 99.00$ m is formed by a concrete deck suspended on a suspension cable of the midspan sag f . The structure was analysed for two arrangements of the suspension cables called **A** and **B**– see Fig.5.2.2. In the option **A** there is a two meter gap between the cable and deck, in the option **B** the cable is connected to the deck at midspan.

A concrete deck of area $A_D = 1.500$ m² and modulus of elasticity $E_D = 36$ GPa was analysed for four values of bending stiffness characterized by moment of inertia:

$$I_D = 0.005 \text{ m}^4, I_D = 0.050 \text{ m}^4, I_D = 0.500 \text{ m}^4, \text{ and } I_D = 5.000 \text{ m}^4.$$

The initial state was determined for three values of the midspan sag f with corresponding areas A_C and modulus of elasticity $E_C = 190$ GPa for the suspension cable formed by strands.

$$\begin{array}{ll} f = L/8 = 12.375 \text{ m} & A_C = 8.490 \cdot 10^{-3} \text{ m}^2 \\ f = L/10 = 9.900 \text{ m} & A_C = 9.905 \cdot 10^{-3} \text{ m}^2 \\ f = L/12 = 8.250 \text{ m} & A_C = 11.886 \cdot 10^{-3} \text{ m}^2 \end{array}$$

The hangers situated at the distance of 3.00 m are formed by bars of the area $A_H = 1.608 \cdot 10^{-3}$ m² and modulus of elasticity $E_H = 210$ GPa.

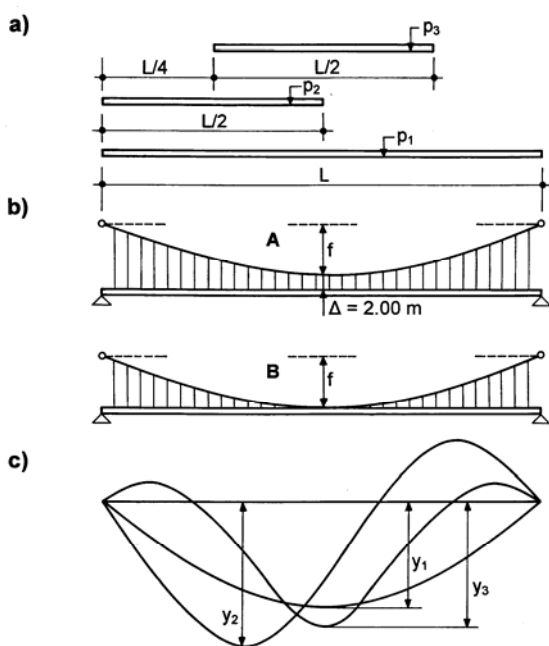
The structure was analysed for three loads:

Load 1 – dead load plus live load 16kN/m situated along the whole deck length.

Load 2 – dead load plus live load 16kN/m situated on one half of the deck length.

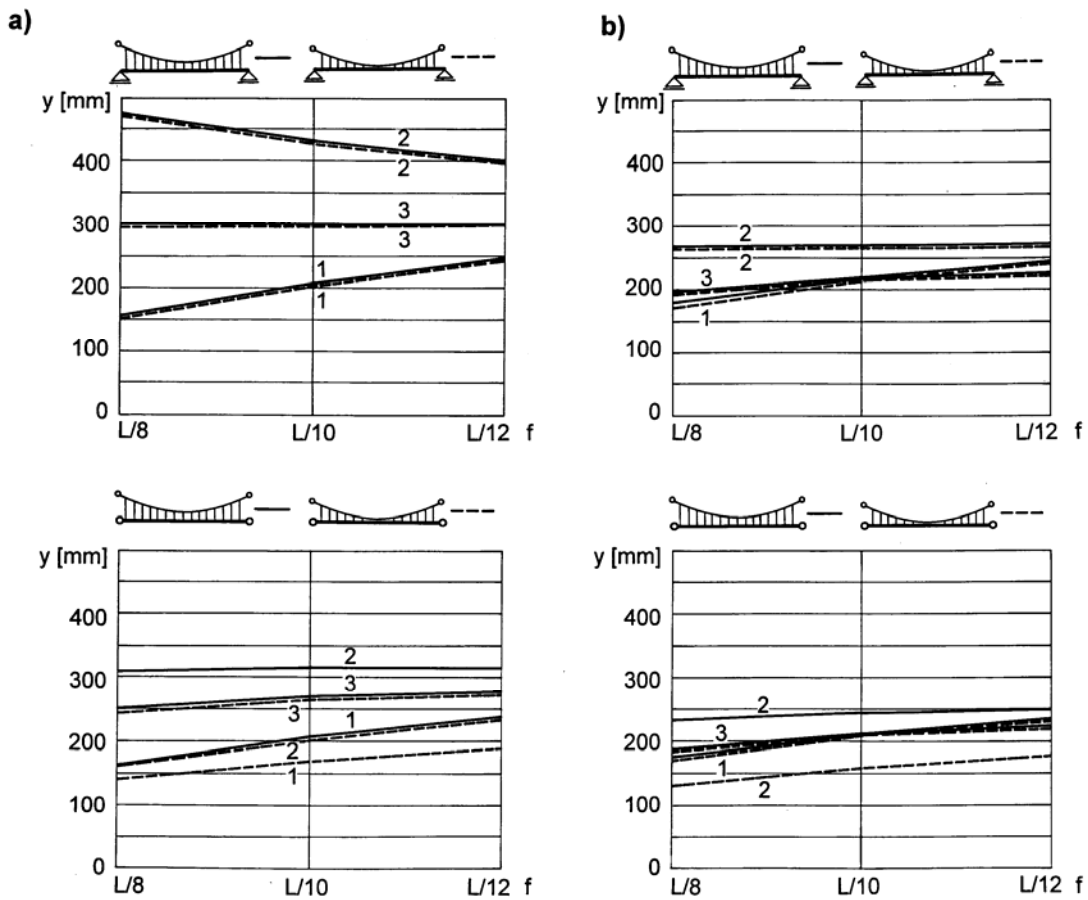
Load 3 – dead load plus live load 16kN/m situated in the central portion of the deck length.

The structure was analysed as a geometrically non linear structure by the program system ANSYS. In the initial state the forces in the cables exactly balanced the dead load. By the analysis the characteristic deformation y_1 , y_2 and y_3 caused by loads 1, 2 and 3 and corresponding internal forces and moments in all structural members were obtained. From the results shown in Fig.5.2.3 it is evident that the maximum reduction of the deflection is caused by



Obz.5.2.2 Parametric study: structure

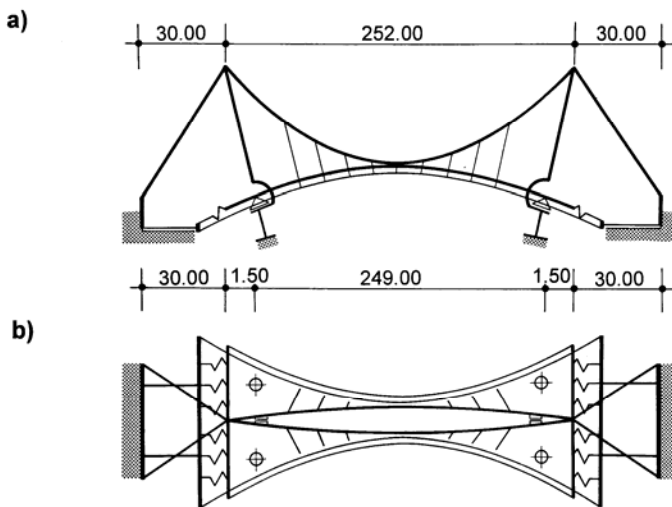
restricting of the horizontal movement at supports. The maximum reduction of the deflection is achieved by a combination of a horizontal fixing and by a connection of the cable with the deck. The different sag of suspension cables influences mainly the amount of steel of the cables.



Obr.5.2.3 Parametric study: deformation of the deck

5.3 EXAMPLE OF THE ANALYSIS

The described modelling and analyses are illustrated on an example of the Vranov Bridge [25] (see Fig.1.2.). The static function of bridge is evident from the Fig.5.3.1 presenting a space calculation model. The towers were modelled as a 3D frame, the suspension cables and hangers as a cable member and the deck as a 3d grid formed by two longitudinal bar members and transverse bar members. The longitudinal members were situated at edge girders, the transverse members at the diaphragms. The structure was stiffened by external tendons that were modelled by cable members and situated parallel with the edge girders.



Obr.5.3.1 Vranov Bridge: calculation model

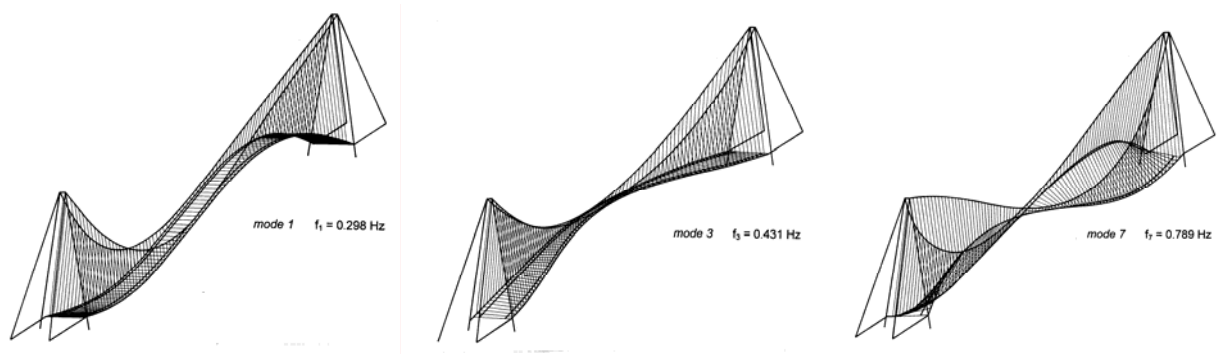


Fig.5.2.6 First vertical, swing and torsional mode

The analyses were done both for the erection and service stage on one calculation model. Since the first 12 natural frequencies corresponding to vertical modes are under the walking frequency of 2 Hz, the bridge proved to be insensitive to pedestrian loading - see Fig.5.2.6. Even the loading imposed by vandals (a group of people trying to make the bridge vibrate in an eigenmode) caused negligible effects with amplitude of several millimeters.

6 CABLE STAYED STRUCTURES

Cable stayed structures have been described in several excellent books [5], [7], [9], [10], [32]. Therefore only additional information about structures formed by slender deck is presented in this chapter.

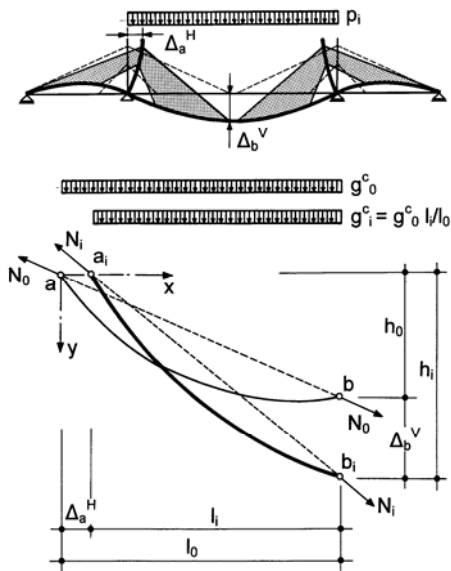
6.1 STRUCTURAL ARRANGEMENT

Cable stayed structures are formed by a slender deck that is suspended on stay cables anchored in the tower and deck. It is possible to anchor back stays in the soil and create totally or partially earth cable stayed structure. But from economical reasons this solution makes sense only in special cases and/or for structures of long spans. The prevailing portion of the cable stayed structures is formed by self anchored systems that stress the footings by vertical reactions only. The cable stayed structures usually do not utilize increasing of the stiffness of the structural system by anchoring of the deck at the abutments. However, the advantage of restricting the horizontal movement at the abutments was demonstrated by the author in his latest designs of the pedestrian bridges that will be built in Eugene, Oregon, USA, and Bohumín, ČR.

6.2 STATIC ANALYSIS

The cable stayed structures can be analysed similarly to suspension structures as geometrically nonlinear structures. The stay cables can be modelled as suspension cables, the towers and deck by 3D bars or shell elements. However, the larger stiffness of the cable stayed structures given by the height of the towers and by an initial tension in the stay cables allows substituting the stay cables by bar elements. If the tension stiffness of the deck is not utilized, the cable stayed structure can be analysed linearly and it is possible to use a superposition of the static effects. Then the structure can be analysed in two steps. In the first step, the stresses due to the dead load and prestress are determined. In the second step the structure is analysed as common structures by linear programs. Since the cable stayed structures usually form progressively erected hybrid systems, the time dependent analysis is mandatory.

The stay cables that are anchored at towers and the deck behave as cables that are loaded by their own weight and by deflection of their supports. Fig.6.2.1 shows deformation of anchor points of the longest stay cable of the Elbe River Bridge [21]. It is evident that a new position of the cable is influenced mainly by a horizontal deformation of the tower and vertical deflection of the deck. Due to these deformations the length of the cables and consequently the stresses in the cables have changed.

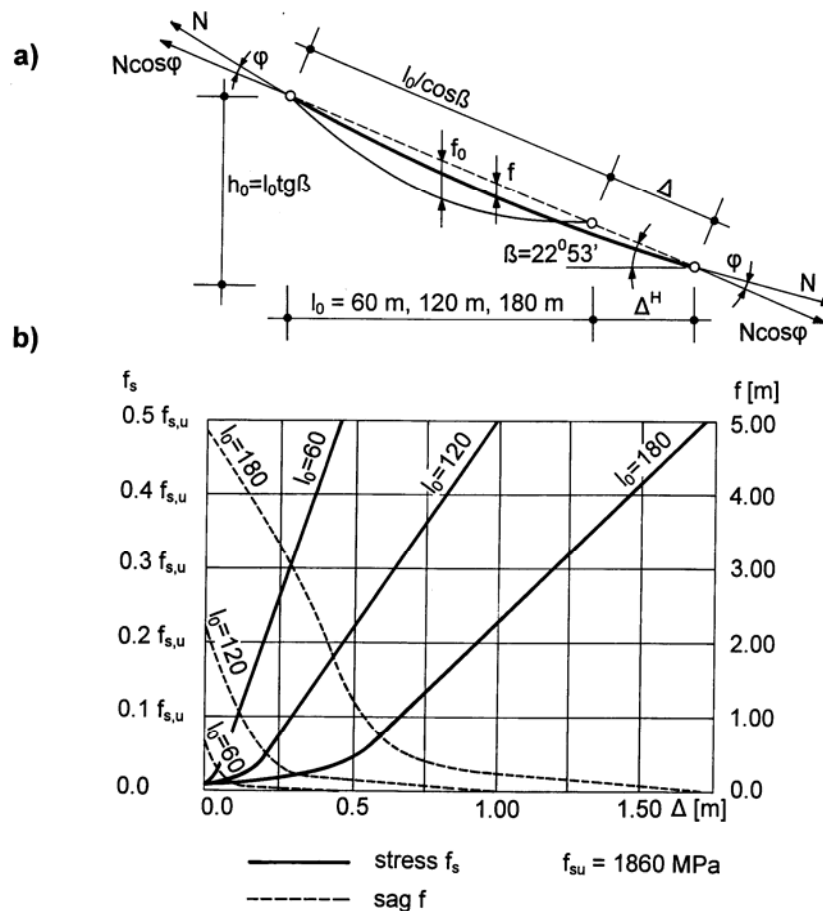


Obr.6.2.1 Static function of the stay cable

For understanding the function of the cable the following study was done. Fig.6.2.2a shows cables of the lengths of $l_0/\cos\beta$ where l_0 is 60, 120 and 180 m. The cable was assembled of 0.6" strands of the modulus of elasticity of $E_s = 190$ GPa. The cables were stressed by an initial stress

$$f_s = 0.005 f_{s,u} = 0.005 \cdot 1,860 = 93.0 \text{ MPa.}$$

Then the cables were loaded by deflection Δ that was step by step increased in increments 0.05 m. The results of the analyses are presented in Fig.6.2.2b where stresses in the cables f_s and corresponding sags f are plotted. It is evident that the studied cables behave nearly linearly (the change of stress is linearly proportional to the change of the deflection) for the stresses $f_s > 0.1 f_{s,u}$. For longer stay cables the initial stresses have to be higher. The non linear behaviour is usually taken into account by using so called Ernst modulus.



Obr.6.2.2 Normal stresses and sag in the stay cable

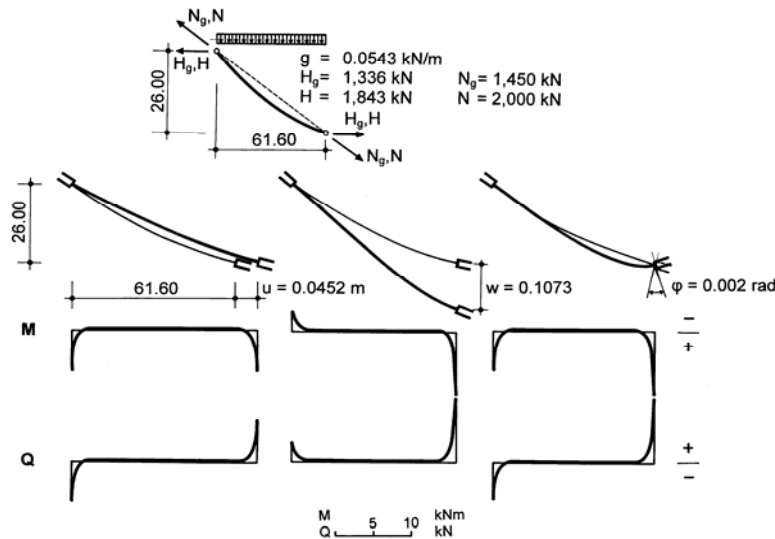
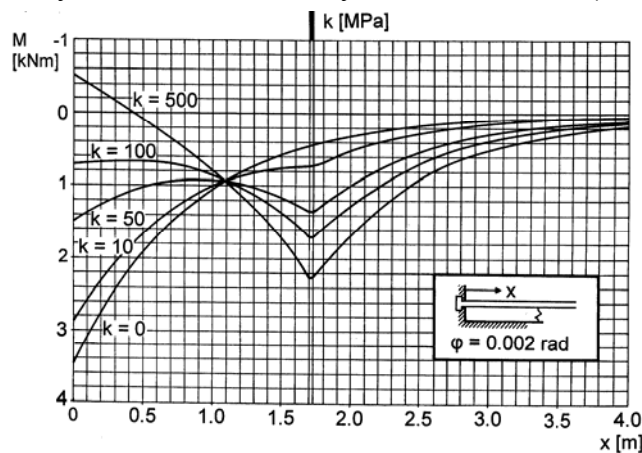


Fig.6.2.3 Bending moment and shear forces in the stay cable

The stay cables are usually fixed into the pylons and deck. Due to their deformations significant bending and shear stresses originate at stay's anchors. Fig.6.2.3 shows the deformations and corresponding shear forces and bending moments that originate due to the design live load in the longest stay cable of the Elbe Bridge [21]. Since corresponding stresses significantly influence the design of the stay cables, it is necessary to develop structural details that reduce them.

Fig.6.2.4 shows a course of the bending moments that originate in the vicinity of their anchors in the stays that were loaded by rotation of deck $\varphi = 0.002$ rad. The stay is - at the distance 1.7 m



6.2.4 Bending of the cable

from anchor - supported by a spring. The spring has different stiffness that varies from 0 to 500 MPa. It is evident that the bending moment can be significantly reduced and the peak of bending moment can be transferred from the anchor to the spring.

This is the reason why modern stay cables are guided by a strong pipe that is ended by a neoprene ring. The neoprene ring, together with the pipe, creates a flexible support - spring - that reduces the local bending moments.

6.3 REDISTRIBUTION OF STRESSES

It is known that a significant redistribution of stresses can occur in structures that change their static system during construction [11], [17]. The significance of this phenomenon is illustrated on an example of a simple cable supported structure. Fig.6.3.1 shows a simple beam of 12 m span, which was after 14 days of curing suspended at midspan on a very stiff stay cable ($E_s A_s = \infty$). Before suspending, a force N was introduced in the cable. The values of N were $N = 0$, $N = R$ and $N = 2R$, where R is a reaction at the intermediate support of a 2 span continuous beam under uniform loading.

The time dependent analysis was performed for the old Morsch and CEB-FIP (MC 90) [2] creep functions. With time, a significant redistribution of bending moments has occurred for $N = 0$ and $N = 2R$. The bending moment diagram is changing towards the diagram of a two span beam.

Concrete is a natural material and therefore the structure tries to behave naturally – as a continuous beam. In this case a larger redistribution of stresses is obtained for the old Mörsh creep function. It is important to realize that for the force $N = R$ there is no redistribution for both creep functions. The structure keeps its shape and the stresses are constant in time [6],[8]. Their values do not depend on the adopted creep function. Since it is difficult to design a structure in which the stresses are changing in time, it is very important to design an initial stage such that the redistribution of stresses is minimal. In case the deck is suspended on arches or pylons, the initial forces in the stay or suspension cables have to be determined from the condition of zero deck deflection at the anchor points.

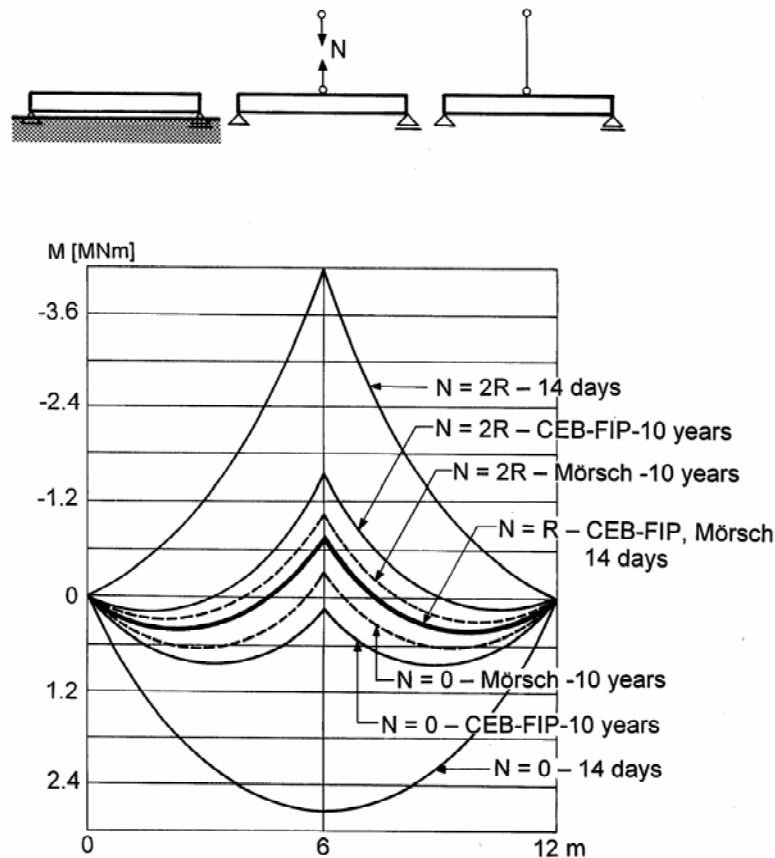


Fig.6.3.1 Redistribution of bending moments

It is evident that the initial force in the stay cable has to correspond to the reaction of a two span continuous beam. Then there is no redistribution of forces in time. However, the cable was vertical and therefore the beam was not compressed. Since the stay cables are inclined, they stress the beam by normal forces. The normal stresses create horizontal deformations that, due to the creep of concrete, increase in time. Also shrinkage of concrete causes horizontal deformations of the deck. Therefore the stay anchor horizontally moves and its initial force is reduced. The change of the stay force causes a redistribution of stresses in the structure.

To quantify this phenomenon, extensive studies were done under the author's control. Here only few results are presented. Fig.6.3.2a shows the same beam that was, after 14 days of curing, suspended at mid-span on a very stiff inclined stay cable ($E_s A_s = \infty$). Before suspending a force

$$N = R / \cos \beta$$

was created at the cable. R is a reaction at the intermediate support of a continuous beam of two spans 2×6 m. The time dependent analysis was performed using CEB-FIP (MC 90) creep

function. In time the bending moments are redistributed from the anchor point to the span; at time $t_{\infty} = 100$ years the moment at the anchor point is app. 60% of the initial moment.

Another analysis was also done on the assumption that there is no shrinkage in the beam. In this case the redistribution is very small – see Fig.6.3.2b.

The time dependent analysis was also done for the structure in which the initial force was increased by 10% - see Fig.6.3.2c. The value of the redistribution of bending moments was similar to the redistribution of moments shown in Fig.6.3.2a, but the final value was closer to the bending moment that corresponds to the force $N = R/\cos \beta$.

Fig.6.3.2d presents the results of the analysis in which the force in the stay cable was adjusted after one year. The redistribution of moments was significantly reduced; at time $t_{\infty} = 100$ years the moment at the anchor point is app. 80% of the initial moment.

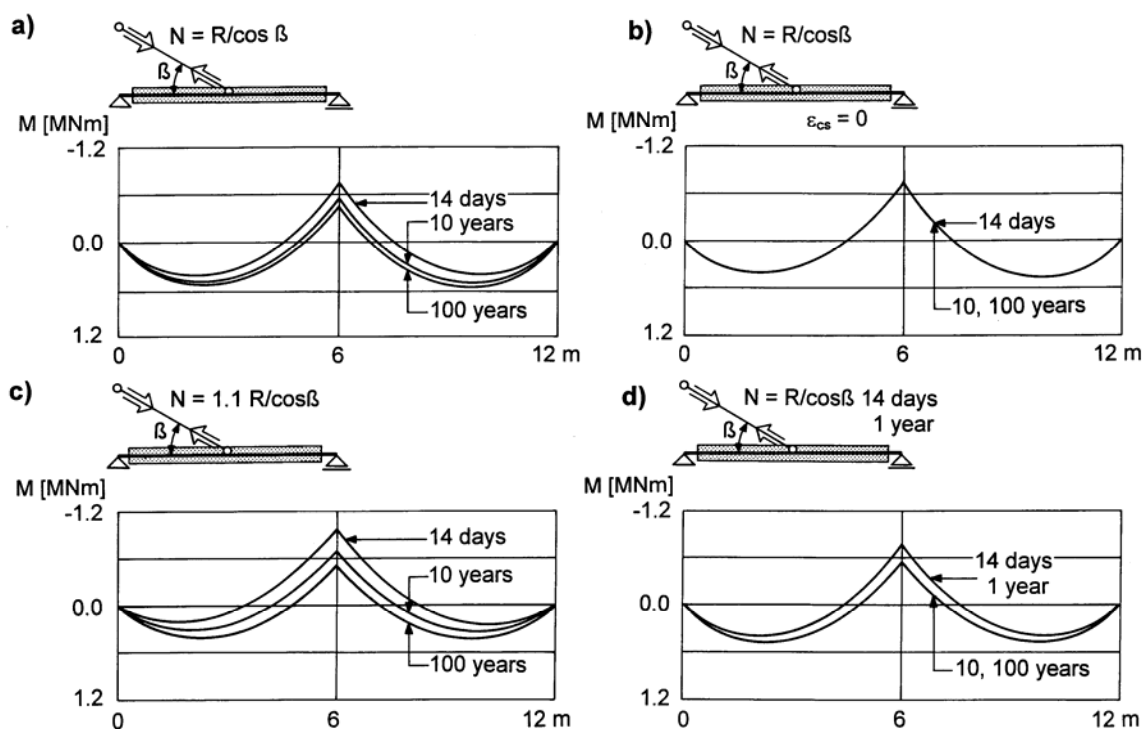


Fig.6.3.2 Redistribution of bending moments

It is evident that the redistribution of moments can reach significant values. However, it is necessary to realize that in the structures with slender deck, which is suspended on multiple stay cables, the bending moments due to the dead load are – compared to the bending moment due to the live load and temperature changes - very small.

To quantify the influence of the redistribution of stresses in actual cable supported structures a cable stayed structure shown in Fig.6.3.3 was studied. The goal of the studies was to determine optimum forces in the stay cables of progressively erected cable stayed structures. The analyses were done for non composite and composite deck of a different stiffness. Here only the results of the analysis done for a slender deck are presented. The parametric study was performed for a symmetrical cable stayed structure with radial arrangement of the stay cables. To eliminate the influence of the tower's stiffness, the towers were modelled as movable bearings that can rotate and move in the horizontal direction of the bridge. Since the stay cables have a symmetrical arrangement, the side spans are stiffened by additional supports.

The structure was analysed for the effects of the dead and live loads given by the Czech standards and for temperature changes $\Delta t = \pm 20^{\circ}\text{C}$. The area of the cables was determined from the conditions of $\max f_s \leq 0.45 f_{s,u}$.

The deck was progressively cast in 6 m long sections. It was supposed that the traveller has a similar arrangement and weight as the traveller used in a construction of the Diepoldsau Bridge [32]. The time dependent analysis was done for a progressive erection in which one segment was completed (moving of the traveller, placing of the reinforcement, casting of the segment and post-tensioning of the stay cable) within 7 days.

The forces in the stay cables were determined in several iterations. In the analysis the structure was several times progressively demounted and erected in such a way that in the final stage shown in Fig.6.3.3 (after the erection of the symmetric cantilevers) the forces in all stay cables were $N_i \cong R_i/\cos \beta_i$. It is evident that after 100 years a significant redistribution of the bending moments has occurred. To quantify the value of the redistribution, bending moments envelopes determined for live load and temperature changes of $\Delta t = \pm 20^\circ\text{C}$ are also shown. It is evident that the dead load moments are – compared to moments due to the live load – very small. Therefore it is evident that the value of the redistribution is not - from the engineering point of view - critical and can be accepted. The redistribution can be also notably reduced if the forces are adjusted after 1 year.

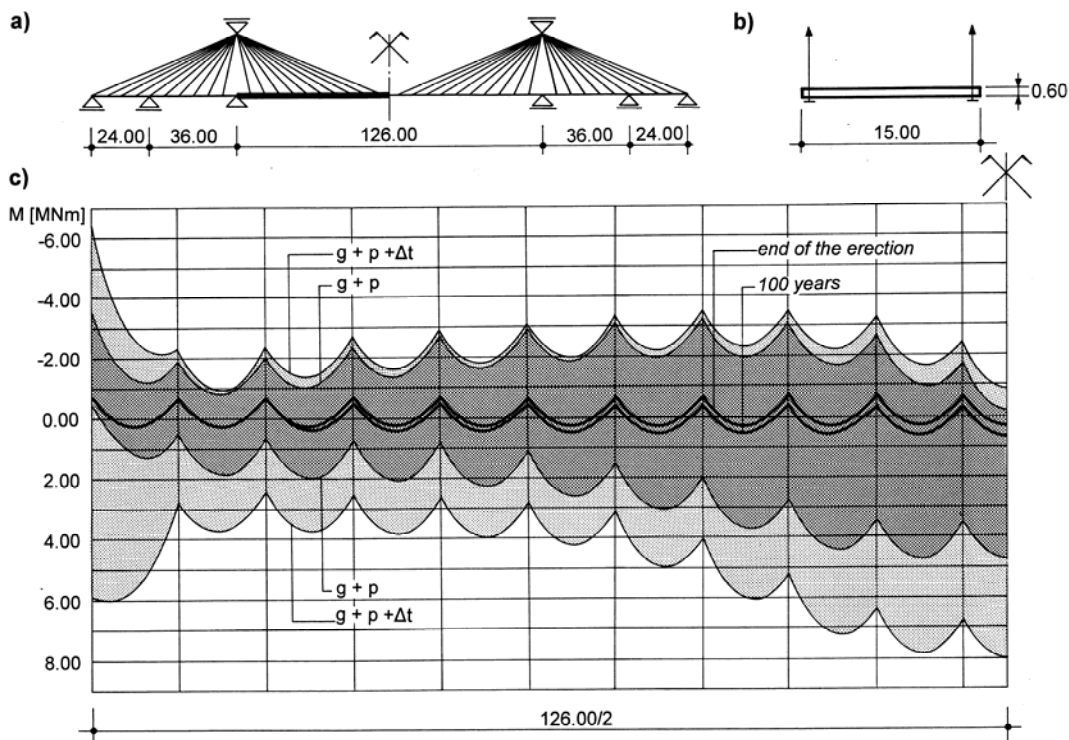


Fig.6.3.3 Redistribution of bending moments in the cable stayed structure

6.4 RESTRICTING OF THE HORIZONTAL MOVEMENT

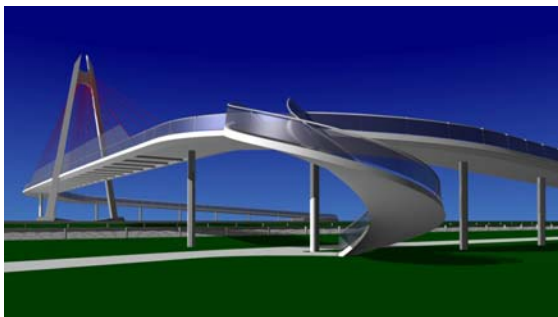


Fig.6.4.1 Eugene Bridge

The advantage of restricting the horizontal movement at the abutments of the cable stayed bridges was recently demonstrated by the author in his latest designs of the pedestrian bridges that will be built in Eugene, Oregon, USA.

The precast deck of the average thickness of 220 mm is fixed into the curved approaches. The approaches function as springs that reduce the horizontal movement of the deck caused by a live load, and – in the same time - allow the movement of the deck due to temperature

changes, creep and shrinkage of concrete. The static analysis has proved that the structure with very slender deck has satisfactory static and dynamic behaviour.

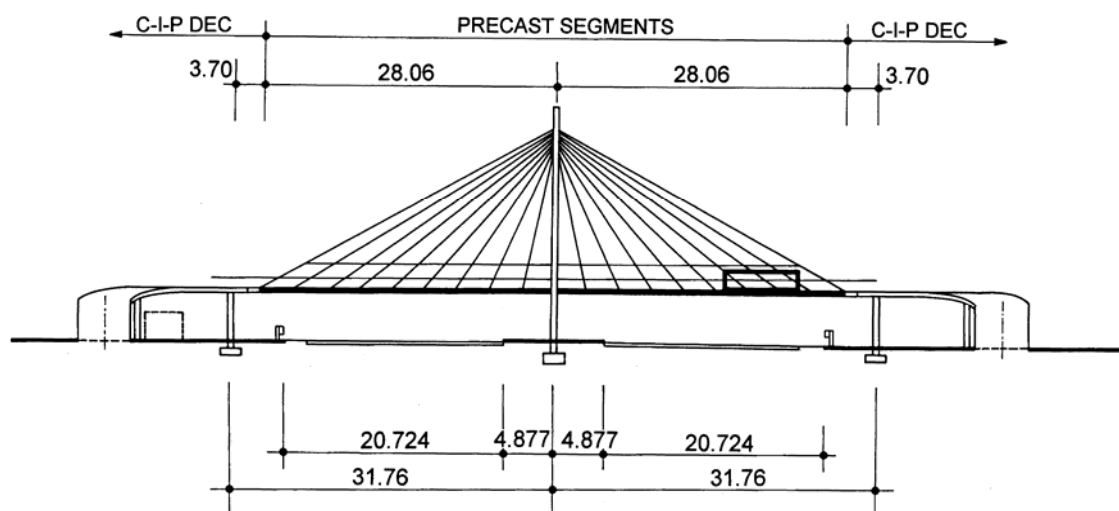


Fig.6.4.2 Eugene Bridge: elevation

7 CONCLUSIONS

Recent designs of the stress ribbon and cable supported structures have confirmed that a slender concrete deck supported by internal and/or external cables can be very efficient. However, their design have to be based on understanding the function of the cables, their tension and bending stiffness and on the understanding of the function of the prestressed concrete deck.

The work explains all important aspects of the design and proves the correctness of the solutions on built structures. The function of the structures was verified by static and dynamic loading tests and by a performance of the bridges during the extremely large floods that occurred in the Czech Republic in 1997 and 2002.

At present, curved bridges formed by a slender concrete deck utilizing a space arrangement of the cables and prestressing tendons are being studied.

REFERENCES

- [1] Bednarski, C.,-Strasky, J.: The Millennium Bridge. L' Industria Italiana del Cemento, N 792 / 2003, Roma, Italy.
- [2] CEB-FIP Model Code 1990. Comité Euro-International du Béton. Thomas Telford. London 1993.
- [3] Eibel,J.- Pelle, K.- Nehse,H.: Zur Berechnung von Spannbandbrücken – Flache Hängebänder. Verner - Verlang, Düsseldorf 1973.
- [4] Endo,T.-Tada K.,Ohashi,H.: Development of suspension bridges - Japanese experience with emphasis on the Akashi Kaiko bridge. Conference: Cable-stayed and suspension bridges. Deauville, France 1994.
- [5] Gimsing, N. J.: Cable Supported Bridges, Concept & Design. John Wiley & Sons. Chichester 1998.
- [6] Leonhardt, F.: Prestressed Concrete. Design and Construction. Wilhelm Ernst & Sons. Berlin1964.
- [7] Leonhardt F. and Zellner W. Cable-stayed bridges. International Association for Bridge and Structural Engineering Surveys, S-13/80, February, 1980.

- [8] Lin, T.Y.,- Burns, N. H.: Design of Prestressed Concrete Structures. John Wiley & Sons. New York 1981.
- [9] Mathivat, J.: The cantilever construction of prestressed concrete bridges. John Wiley & Sons. New York 1983.
- [10] Menn, C.: Prestressed Concrete Bridges. Birkhäuser Verlag, Basel 1990.
- [11] Navrátil, J.: Time-dependent Analysis of Concrete Frame Structures (in Czech), Building Research Journal (Stavebnický časopis), No. 7, Vol. 40, 1992.
- [12] Ostenfeld, K.H.: From Little Belt to Great Belt. Conference: Cable-stayed and suspension bridges. Deauville, France 1994.
- [13] Podolny, W. Jr. - Scalzi, J.B.: Construction and Design of Cable Stayed Bridges. John Wiley & Sons. New York 1976.
- [14] Redfield, C.- Strasky, J.: Stressed ribbon pedestrian bridge across the Sacramento river in Redding, Ca, USA, L'Industria Italiana del Cemento N 663 /1992. Roma, Italy.
- [15] Scott, R.: In the Wake of Tacoma. ASCE Press. Resno 2001.
- [16] Schlaich, J.- Schober, H.: A suspended pedestrian bridge crossing the Neckar river near Stuttgart Conference: Cable-stayed and suspension bridges. Deauville, France 1994.
- [17] Smerda, Z.- Kristek, V.: Creep and Shrinkage of Concrete Elements and Structures. Elsevier. Amsterdam 1988.
- [18] Strasky, J.- Pirner, M.: DS-L Stress ribbon footbridges. Dopravni stavby, Olomouc, Czechoslovakia 1986.
- [19] Strasky, J.: Precast stress ribbon pedestrian bridges in Czechoslovakia. PCI JOURNAL, May-June 1987.
- [20] Strasky, J.: Static analysis of the prestressed band. Conference 'Tension Structures'. Piestany, Czechoslovakia 1990.
- [21] Strasky, J.: Design and construction of cable-stayed bridges in the Czech Republic. PCI JOURNAL, November-December 1993.
- [22] Strasky, J.: Architecture of bridges as developed from the structural solution. FIP'94 - International Congress on Prestressed Concrete. Washington 1994.
- [23] Strasky, J.: Stress-ribbon pedestrian bridges. International Bridge Conference. Pittsburgh 1999.
- [24] Strasky, J.: The power of prestressing. Structural Concrete. London 2003. ISSN 1464-4177, Thomas Telford and fib. London 2003, pp.25-43.
- [25] Strasky, J.: Pedestrian Bridge Suspended over Lake Vranov, in the Czech Republic. L'Industria Italiana del Cemento, N 736 / 1998, Roma, Italy.
- [26] Strasky, J.-Navratil, J.-Susky, S: Applications of Time-Dependent Analysis in the Design of Hybrid Bridge Structures. PCI Journal, July/August 2001.
- [27] Strasky, J.: Long-Span, Slender Pedestrian Bridges. Concrete International, February 2002, pp.42-48.
- [28] Strasky, J.: Stress ribbon and suspension pedestrian bridges. The World of Bridges, Venice, Italy 2001.
- [29] Jiri Strasky: Stress ribbon and cable supported pedestrian bridges. ISBN: 0 7277 3282 X. Thomas Telford Publishing, London 2005.
- [30] Timoshenko, S.P.- Goodier, J.N.: Theory of Elasticity. McGraw-Hill. New York 1970.
- [31] Troyano, L.F.: Bridge Engineering. A Global Perspective. Thomas Telford Publishing, London 2003.
- [32] Walther, R.- Houriet, B.- Walmar, I.- Moïa, P.: Cable Stayed Bridges. Thomas Telford Publishing, London, 1998.